ELSEVIER

Solid State Nuclear Magnetic Resonance 6 (1996) 1–29

SOLID STATE
Nuclear Magnetic
Resonance

Review

Multinuclear solid-state NMR studies of acidic and non-acidic hydroxyl protons in zeolites

Michael Hunger

Institute of Chemical Technology I, University of Stuttgart, D-70550 Stuttgart, Germany

Received 1 April 1995; accepted 11 June 1995

Abstract

Among the variety of experimental techniques used for the characterization of aluminosilicate and aluminophosphate-based molecular sieves, NMR spectroscopy has the advantage of providing detailed information on local bonding and solid-state interactions. In the last 15 years, NMR has been used to study zeolitic frameworks, catalytic active centres, adsorbed probe molecules and their chemical interactions. This paper reviews multinuclear solid-state NMR studies of Brønsted acid sites in zeolites. The main topics are the formation, accessibility and localization of hydroxyl protons, dehydroxylation of zeolites, the interaction of hydroxyl protons with probe molecules, and the geometry and parameters of the local structure of OH groups in these materials.

Keywords: Hydroxyl group; zeolite; Brønsted acidity; Local structure

1. Introduction

Crystalline aluminosilicate zeolites and silicoaluminophosphate molecular sieves possess well-defined intracrystalline systems of channels and cavities. Acid centres on the extensive (about 800 $m^2\ g^{-1}$) inner surfaces make zeolites of interest in the field of heterogeneous catalysis [1–3]. Hydroxyl protons which act as Brønsted acid sites are located on oxygen bridges connecting tetrahedrally co-ordinated silicon and aluminium atoms. These protons compensate the negative framework charges introduced by the tetrahedrally co-ordinated aluminium. These OH groups are known as structural or bridging OH groups (SiOHAl). "Silanol" (SiOH) groups are located on the outer surface of zeolitic particles or at framework defects. The removal of aluminium atoms from the zeolitic framework by hydrothermal treatment is the most important origin of these defects. The extent of healing of the defects by the migration of silicon from other parts of the crystal and the formation of silanol groups depend on the conditions of dealumination. In addition, there is evidence for the formation of OH groups associated with extra-framework aluminium species. As all these types of OH group influence the catalytic and sorptive properties of zeolites, their study is essential for the successful industrial application of zeolites as acidic catalysts [4–6].

A number of quantum chemical studies reported in the last 5 years [7–14] have addressed the local structure and chemical behaviour of

0926-2040/96/$15.00 © 1996 Elsevier Science B.V. All rights reserved
SSDI 0926-2040(95)01201-X

Brønsted sites in zeolites. For SiOHT groups with T = B, Al, Si or P and only oxygen atoms in the first co-ordination sphere of the silicon and T atoms, a relation between the intrinsic acid strength of isolated hydroxyl protons, the deprotonation energy ΔE_{DP}, and the ^{1}H shift has been found [12]. In addition, quantum chemical studies have demonstrated that protonation and deprotonation of zeolitic frameworks leads to a local change in the geometry of the Si–O–Al bridges [9], which respond to the attack of hydroxyl protons by a readjustment of bonds. Calculations by Teunissen et al. [14] indicate a relaxation of the zeolite framework in the presence of ammonia. Recently, quantum chemical studies [7,13,15,16] have been done to investigate the interaction of bridging OH groups and methanol molecules in zeolites; the results suggest the formation of hydrogen-bonded complexes.

The characterization of acidic OH groups in zeolites by ^{1}H magic angle spinning (MAS) NMR was first discussed by Freude and co-workers [17,18]. The acidity of zeolites and solid surfaces is described by two independent quantities: (i) the acid strength, defined as the ability of the hydroxyl proton to protonate an adsorbed molecule; and (ii) the concentration of hydroxyl protons which are accessible to adsorbed molecules. The latter can be derived from the ^{1}H MAS intensities of the hydroxyl protons accessible to probe molecules. The acid strength of OH groups which are not involved in hydrogen bonding or other chemical interactions correlates with the ^{1}H chemical shift; a large chemical shift corresponds to a high acid strength. However, in unknown systems it may be difficult to decide whether the observed ^{1}H shift of the hydroxyl protons originates from the intrinsic acid strength or from the formation of hydrogen bonds. ^{1}H MAS NMR studies of probe molecules adsorbed at acidic OH groups are therefore important for the characterization of Brønsted acidity (see Section 3). Ernst et al. [19] have suggested the use of the quadrupole coupling constant of OD groups in zeolites (see Section 4) as a quantitative measure of acid strength. For a general review of NMR studies of the Brønsted and Lewis acidity of zeolites, the reader is referred to Refs. [20–22]. The resolution of solid-state ^{1}H MAS NMR spectra of OH groups in inorganic solids and zeolites is discussed in Refs. [23–25].

This paper reviews the application of solid-state NMR to the study of OH groups in dehydrated zeolites, the formation and dehydroxylation of the H-form of zeolites (Section 2), the mobility of hydroxyl protons (Section 3), the interaction of hydroxyl protons with probe molecules (Section 4), their location in cavities and channels (Section 5) and the local structure of OH groups (Section 6). We show that the high sensitivity of NMR to local bonds and solid-state interactions makes the technique useful for the derivation of information complementary to that obtainable by infra-red (IR) [27,28] and diffraction techniques [29,30].

2. Characterization and modification of hydroxyl groups in zeolites

2.1. Assignment of ^{1}H MAS NMR lines in dehydrated zeolites

The first solid-state ^{1}H NMR studies of dehydrated zeolites were carried out in 1982 at a magnetic field $\boldsymbol{B}_0$ of 1.4 T with single-pulse excitation [17]. The linewidths of the peaks from the OH groups were about 1 kHz. Fields $\boldsymbol{B}_0$ of ≥ 7 T greatly decrease the residual linewidth to about 250 Hz [18,31]. With MAS frequencies ν_{rot} of ≥ 10 kHz, the resolution of ^{1}H MAS NMR spectra of dehydrated zeolites corresponds to that recorded with CRAMPS [24,31].

The ^{1}H resonance positions of hydroxyl protons in zeolites are in the chemical shift range 0–6 ppm. Hydroxyl groups at Mg^{2+} cations located on site SII in the supercages of zeolite Y (Fig. 1) appear at about 0 ppm (Fig. 2(a)) [32]. The line of AlOH groups (MeOH) on the outer surface of dehydrated γ-Al_2O_3 and η-Al_2O_3 was found at about -0.2 ppm [33]. Silanol groups (SiOH) give lines in the range 1.3–2.2 ppm (Figs. 2 and 4) [35].

The ^{1}H shifts of bridging OH groups in supercages (SiO1HAl groups in zeolite Y, structure type FAU [117]) or channels of the zeolite frame-

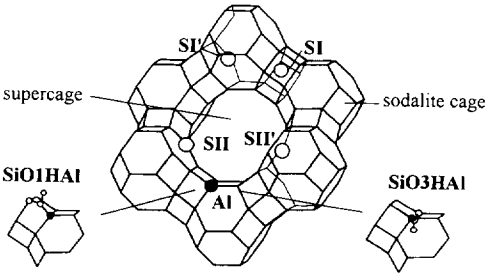


Fig. 1. Structure of zeolite Y with bridging OH groups pointing into the supercage (SiO1HAl) and the sodalite cages (SiO3HAl) and cation positions in the supercage (SII), the sodalite cages (SI', SII') and the hexagonal prisms (SI).

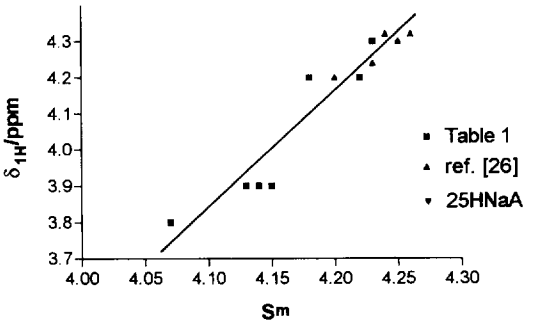


Fig. 3. ^{1}H NMR shifts δ_{1H} of bridging OH groups in the supercages and channels of aluminosilicate-type zeolites as a function of the mean Sanderson electronegativity S^m [38] given in columns 6 and 7 of Table 1 and in Ref. [26].

works depend on the framework Si/Al ratio [35,36] and, therefore, on the mean electronegativity of the zeolitic framework [26]. The shift values cover a range of 3.8–4.3 ppm. Fig. 3 shows the chemical shift values δ_{SiOHAl} of free SiOHAl groups in the supercages or channels of zeolites (column 7, Table 1; Refs. [26,35,37]) as a function of the mean Sanderson electronegativities S^m [38] of the frameworks (column 5, Table 1; Ref. [26]). The values of S^m were derived as the geometric average of the Sanderson electronegativities S_i of atoms i ($S_{Al} = 2.22$, $S_O = 5.21$, $S_{Si} = 2.84$ and $S_H = 3.55$) according to their number in the unit cell. Fig. 3 also indicates that an increase in the mean electronegativity of the zeolitic framework causes an increase in the chemical shift δ_{1H} of the SiOHAl groups in supercages and channels. Note the significant deviation in the shift δ_{1H} of the bridging OH groups in zeolite 25HNaA (structure type LTA [117]), which may be caused by the location of the bridging OH groups in eight-membered oxygen rings (see below).

Low-field ^{1}H MAS lines at about 4.8 ppm originate from hydroxyl protons of bridging OH groups located in small cavities or six-membered

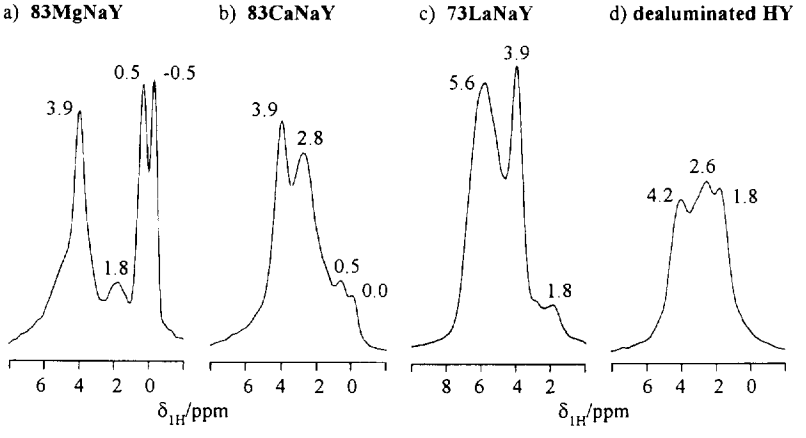


Fig. 2. ^{1}H MAS spectra of zeolites 83MgNaY (a) [32], 83CaNaY (b) [32] and 73LaNaY (c) [151] calcined at 433 K, and of dealuminated zeolite HY (d) [44] calcined at 673 K. The spectra in (a), (b) and (d) were recorded at 300.13 MHz with a MAS frequency of $\nu_{rot} = 3$ kHz. The spectrum in (c) was measured at 400.13 MHz with a MAS frequency of $\nu_{rot} = 10$ kHz.

oxygen rings (columns 3 and 7, Table 1), e.g. from SiO3HAl groups in the sodalite cages of zeolite Y. Fourier-transform IR (FTIR) and ^{1}H MAS studies of zeolites HY and HEMT have shown that a low-field ^{1}H MAS shift and a simultaneous decrease in the IR wavenumbers of hydroxyl protons of bridging groups (see Fig. 1) can be explained by weak hydrogen bonding [39]. Using time-resolved vibrational spectroscopy, Brugmans et al. [40] found mean vibrational lifetimes of 223 and 42 ps for the protons of the SiO1HAl and SiO3HAl groups in dehydrated zeolite HY, respectively. This indicates a weak hydrogen bond of the O–H oscillator of SiO3HAl groups.

A quantitative relation between the O–O distance of the hydrogen bonds (d_{OH-O}, pm) and the low-field shift ($\Delta\delta_{1H}$, ppm) of the ^{1}H resonance positions of metal OH groups in calcium phosphates was empirically derived by Yesinowski and Eckert [41]:

$$\Delta\delta_{1H} = 79.05 - 0.255 d_{OH-O} \quad (1)$$

Hydroxyl protons of the CaOH groups located in sodalite cages of zeolites CaNaY show a low-field shift $\Delta\delta_{1H}$ from about 0 ppm (MeOH, see above) to 2.8 ppm (Fig. 2(b)) [32]. X-ray diffraction (XRD) studies show that OH groups are bonded to calcium cations ($CaOH^+$) located at SI′ sites in the sodalite cages (Fig. 1) of zeolite CaNaY with an O–O distance to the next-nearest framework oxygen atom of 0.297 nm [42]. According to Eq. (1), the low-field shift of $\Delta\delta_{1H} = 2.8$ ppm corresponds to an OH $\cdots$ O distance d_{OH-O} of 0.295 nm, which is in good agreement with the XRD value. In zeolite LaNaY a low-field shift of the ^{1}H lines of $LaOH^{2+}$ groups $\Delta\delta_{1H}$ of about 5.6 ppm was observed (Fig. 2(c)) [151]. In the spectra of dealuminated zeolites HY [44], H-mordenite (structure type MOR) [35] and HZSM-5 (structure type MFI) [45,46], the lines of the hydroxyl protons on extra-framework aluminium species appear at chemical shifts in the range 2.6–3.6 ppm (Fig. 2(d)). The comparison of these resonance positions with those of AlOH groups on the outer surface of aluminium oxides [33] yields a low-field shift $\Delta\delta_{1H}$ of about 3 ppm, indicating the formation of hydrogen bonds between the hydroxyl protons attached to extra-

Table 1
Structural data [117], molar ratios of T atoms [37], mean Sanderson electronegativities S^m [38] of aluminosilicate frameworks, chemical shifts [37], δ_{1H}, of bridging OH groups and H-Al distances [37], r_{HAl}, in the local structure of bridging OH groups derived from ^{1}H MAS NMR sideband patterns.

Zeolite	Structure type [a]	Oxygen rings [a]	n_{Si}/n_{Al}	$n_{Si}/n_{Al+Si+P}$	S^m	δ_{1H} (ppm)	r_{HAl} [b] (nm)
25HNaA	LTA	8-membered	1.0		4.06	4.0	0.238
50HNaX	FAU	12-membered	1.4		4.07	3.8	0.246
52HNaY	FAU	12-membered	2.6		4.13	3.9	0.250
90HNaY	FAU	12-membered	3.5		4.14	3.9	0.250
		6-membered				4.8	0.236
37HKERI	ERI	8-membered	2.9		4.15	3.9	0.246
HM	MOR	12-membered	7.1		4.18	4.2	0.248
HZSM-5/1	MFI	10-membered	15.0		4.22	4.2	0.250
HZSM-5/2	MFI	10-membered	26.0		4.23	4.3	0.246
SAPO-5	AFI	12-membered		0.036		3.8	0.252
		6-membered				4.8	0.236
SAPO-17	ERI	8-membered		0.021		3.7	0.242
		8-membered				4.0	0.240
SAPO-34	CHA	8-membered		0.114		3.8	0.242
SAPO-37	FAU	12-membered		0.121		3.8	0.250
		6-membered				4.3	0.234

[a] See Ref. [117].
[b] Accuracy of 0.002 nm.

framework aluminium species and neighbouring oxygen species [44,45].

A summary of the ^{1}H NMR shifts of hydroxyl protons in dehydrated zeolites is given in Table 2. Using an empirically derived relation [47]

$$\delta_{1H}\ (\text{ppm}) = 42.2 - 0.01\nu_{OH}\ (\text{cm}^{-1}) \qquad (2)$$

the values of the ^{1}H shifts δ_{1H} of the OH groups in zeolites can be estimated from the wavenumbers of their IR stretching vibrations ν_{OH}. No suitable correlation was found between the ^{1}H shift values and the wavenumbers of the IR stretching vibrations of cationic OH groups in zeolites MgNaY and CaNaY.

2.2. Studies of hydrated zeolites

^{1}H MAS NMR studies of hydrated zeolites A, X, Y, ZSM-5 and mordenite have been reported by Kasai and Jones [48]. For hydrated Na-form zeolites, lines of physisorbed water molecules were found in the range of chemical shifts between 3.5 ppm (NaZSM-5) and 4.9 ppm (NaA). ^{1}H MAS spectra of mordenites exchanged with group IA and IIA cations consist of lines at resonance positions between 4.0 ppm for the rubidium-exchanged sample and 4.8 ppm for the magnesium-exchanged sample. In the ^{1}H MAS spectra of hydrated zeolite HZSM-5, Scholle et al. [49,50] found broad lines at about 6 ppm, and explained these as being due to water molecules adsorbed on Brønsted sites. However, as the chemical shifts of bridging OH groups in zeolite HZSM-5 and of bulk water molecules are 4.3 ppm [35,37] and 4.9 ppm [48], respectively, only a rapid exchange of protons between OH groups, water molecules and hydroxonium ions at about 13 ppm [51–53] can cause a line at the resonance position of about 6 ppm (see Section 3). In the ^{1}H MAS spectra of fully hydrated gallosilicate zeolites ZSM-5 (sturcture type MFI), Challoner et al. [54] found lines at 2.1 and 4.8 ppm which originate from water molecules exchanging with silanol groups and Brønsted sites, respectively. Dehydration of gallosilicate zeolite ZSM-5 produced a high-field shift of the above-mentioned lines to resonance positions of 1.7 and 4.0 ppm, respectively. As these chemical shift values agree with those observed for dehydrated HZSM-5 [54], the authors suggest that the acid strengths of the OH

Table 2
^{1}H NMR shifts and assignments of OH groups in dehydrated zeolites

^{1}H NMR shift, δ_{1H} (ppm)	Abbreviation	Type of hydroxyl group	Refs.
−0.5 to 0.5	MeOH	Metal or cation OH groups in large cavities or at the outer surface of particles	32, 33
1.3–2.2	SiOH	Silanol group at the external surface or at lattice defects	18, 35, 37
2.6–3.6	AlOH	OH groups bounded to extra-framework aluminium species located in cavities or channels involved in hydrogen bonds	44–46, 59
2.8–6.2	CaOH, AlOH, LaOH	Cationic OH groups located in sodalite cages of zeolite y and in channels of ZSM-5 involved in hydrogen bonds	32, 58, 59
3.8–4.3	SiOHAl, SiO1HAl [a]	Bridging OH groups in large cavities or channels of zeolites	35, 37
4.6–5.2	SiOHAl, SiO3HAl [a]	Bridging OH groups in small channels and cages of zeolites	35, 37
6.1–7.0	SiOHAl	Disturbed bridging OH groups in zeolite HZSM-5 and Hβ	26, 75–77, 150

[a] Assignment of bridging OH groups in faujasite-type zeolites.

groups in gallosilicate and aluminosilicate zeolite ZSM-5 are comparable.

2.3. Formation of OH groups

Zeolites exchanged with multivalent cations possess strong intracrystalline electric fields. The formation of cationic OH groups and bridging OH groups by the dissociation of water molecules in these electric fields is decribed by the mechanism of Hirschler and Plank [56,57]. In Ref. [32], ^{1}H MAS NMR was used for the quantitative study of the formation of hydroxyl protons due to water adsorption on dehydrated zeolites MgNaY and CaNaY. After adsorption of water, a thermal treatment at 473–673 K was carried out. The concentrations of cationic OH groups and bridging OH groups determined by the ^{1}H MAS intensities were always in a ratio of about 1:1 [32], which corresponds to the reaction scheme:

$$2(\equiv Si{-}O{-}Al^{-}\equiv) + Me(H_2O)_n^{2+} \leftrightarrow \equiv Si{-}O{-}Al^{-}\equiv + Me(OH)^{+} + \equiv Si{-}OH{-}Al\equiv + (n-1)H_2O$$

According to this scheme, the hydrolysis of bivalent cations in zeolites MgNaY and CaNaY produces one cationic OH group and one bridging OH group per dissociated water molecule. After thermal treatment at 473–673 K, a simultaneous decrease in the ^{1}H MAS intensities of the cationic OH and bridging OH groups was observed, which indicates the reversibility of the mechanism proposed by Hirschler and Plank. For zeolite LaNaY, a maximum concentration of bridging OH groups occurs after dehydration at 450 K [58]. The hydrolysis of aluminium cations was studied in zeolite ZSM-5 exchanged with $Al(NO_3)_3$ [59]. After dehydration of zeolite AlZSM-5 at 473 K and subsequent adsorption of water, there was a strong increase in the intensity of the line for the AlOH groups, at a chemical shift of 2.8 ppm. As observed for zeolites MgNaY and CaNaY, dehydration of zeolite AlZSM-5 at 473–673 K is accompanied by a decrease in the concentration of AlOH and bridging OH groups [59].

The occupation numbers of the proton sites at the Si–O1–Al and Si–O3–Al bridges in dehydrated zeolites HNaY were first determined by Olson and Dempsey [60] and Mortier et al. [61] using XRD. Applying neutron diffraction, these quantities were verified by Jirak et al. [62] and

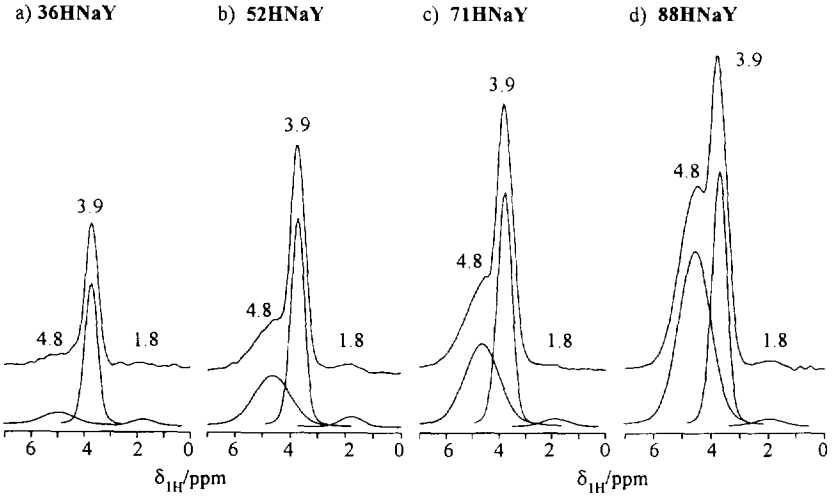


Fig. 4. ^{1}H MAS spectra of calcined (673 K) zeolites HNaY (Si/Al = 2.6) after exchange of (a) 36%, (b) 52%, (c) 71% and (d) 88% of sodium cations by ammonium ions [151]. The spectra were recorded at 400.13 MHz with a MAS frequency of ν_{rot} = 12 kHz. The individual peaks used for the simulation are shown below the spectra.

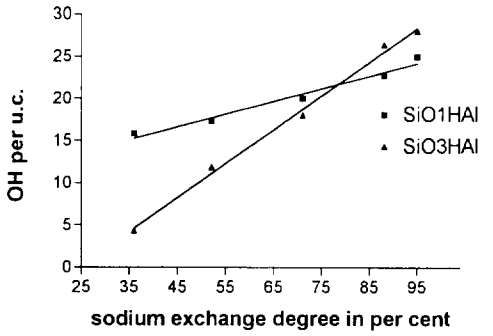


Fig. 5. Concentrations of bridging OH groups in the supercages (line at 3.9 ppm) and the sodalite cages (line at 4.8 ppm) of dehydrated zeolites HNaY as function of the degree of exchange of sodium cations. The values for 36HNaY, 52HNaY, 71HNaY and 88HNaY were determined by deconvolution of the ^{1}H MAS spectra shown in Fig. 4. The values for 95HNaY were taken from Ref. [64].

Czjzek et al. [63]. For a zeolite HNaY prepared by exchange of 95% of Na^{+} cations by NH_4^{+} ions and a subsequent calcination (denoted by 95HNaY), the populations of proton sites in supercages (SiO1HAl) and of proton sites in sodalite cages (SiO2HAl, SiO3HAl) of 28.6 and 24.5 OH/u.c., respectively, were derived [63]. Fig. 4 shows the ^{1}H MAS spectra of dehydrated zeolites HNaY (Si/Al = 2.56) with degrees of sodium exchange of 36% (36HNaY), 52% (52HNaY), 71% (71HNaY) and 88% (88HNaY). The decompositions of the spectra were carried out using the lines of SiOH groups at 1.8 ppm, SiO1HAl groups at 3.9 ppm and SiO3HAl groups at 4.8 ppm. The concentrations of SiO1HAl and SiO3HAl groups as a function of the degree of sodium exchange are shown in Fig. 5. The population numbers of the proton sites in zeolite HNaY with 95% sodium exchange were taken from Ref. [64]. Fig. 5 shows that degrees of sodium exchange of up to 25% cause exclusive formation of SiO1HAl groups in the supercages. For degrees of exchange above 25% there is a linear increase in the concentration of SiO3HAl groups in the sodalite cages.

^{1}H studies of realuminated and rehydroxylated zeolite HNaY have been carried out on samples which were hydrothermally dealuminated at 800 K, treated with an aqueous solution of KOH, ammonium exchanged and calcined at. 673 K [65]. ^{1}H MAS of the sample after calcination shows a doubling of the concentration of bridging OH groups in comparison to the dealuminated parent zeolite, indicating the incorporation of a corresponding number of aluminium atoms into the zeolitic framework. This result is supported by ^{29}Si MAS NMR which shows a decrease in the framework Si/Al ratio from 5.1 to 2.9 and a redistribution of framework aluminium in the realuminated zeolite HNaY [65]. Comparable results have been obtained for hydrothermally dealuminated zeolite HZSM-5 treated with an aqueous solution of NaOH [66].

2.4. Dehydroxylation and hydrothermal treatment of zeolites

Quantitative multinuclear solid-state NMR studies of the dehydroxylation mechanism of zeolite HY have been performed by Freude et al. [67]. Using external ^{1}H and ^{27}Al intensity standards, the concentrations of bridging OH groups and tetrahedrally co-ordinated framework aluminium atoms of zeolite 88HNaY calcined at 573–873 K were determined. The number of bridging OH groups that were dehydroxylated during the thermal treatment was found to be equal to the number of tetrahedrally co-ordinated aluminum atoms released from the zeolite framework. These results disproved the mechanism of dehydroxylation and dealumination proposed by Uytterhoeven et al. [68], who suggested the formation of one three-coordinated framework aluminium atom after dehydroxylation of two bridging OH groups.

Vega and Luz [69] and Shannon et al. [70] applied ^{1}H and ^{29}Si NMR to characterize the nature of OH groups in calcined and steamed zeolite HRHO (structure type RHO). After calcination of zeolite HK-erionite (structure type ERI) [70,71], ^{1}H MAS lines of bridging OH groups in the shift range 3.4–3.9 ppm and of AlOH groups in the range 2.4–2.6 ppm were observed. According to the authors, OH groups at extra-framework

aluminium species were formed due to dealumination of the zeolite framework. Clarke et al. [72] investigated the effect of rehydration on dealuminated and dehydrated zeolite HNaY. After gradual adsorption of water molecules, the ratio of the concentration of AlOH groups at 3 ppm to extra-framework aluminium atoms reached a value of 1.7 [72]. This was explained as being due to the hydrolysis of the extra-framework aluminium species. ^{1}H studies of dealuminated zeolites HNaY, H-mordenite and HZSM-5 have been reported by Lohse et al. [44], Freude et al. [35] and Engelhardt et al. [45], respectively.

Solid-state NMR studies of the relationship between hydrothermal treatment and *n*-hexane cracking activity were carried out using a zeolite HZSM-5 (Si/Al = 15) [46,73,74]. After hydrothermal treatment at 813 K with a water vapour pressure of 6.6 kPa the rate constant of *n*-hexane cracking increased by a factor of 2.7 in comparison to the parent sample. ^{1}H MAS NMR showed a 50% decrease in the concentration of bridging OH groups. This dehydroxylation was found to be coupled with the appearance of ^{27}Al MAS lines of octahedrally ($Al^{o\text{-}ex}$) and tetrahedrally ($Al^{t\text{-}ex}$) co-ordinated extra-framework aluminium species at about 60 and 30 ppm, respectively. The enhanced catalytic *n*-hexane cracking activity was explained in terms of a simultaneous interaction of *n*-hexane with both bridging OH groups and extra-framework aluminium species [46]. However, it is important to note that recent NMR studies of dehydrated zeolites HZSM-5 [26,75–77] indicate the presence of yet another type of OH group. Apart from the line from bridging OH groups at 4.3 ppm, an additional broad line in the chemical shift range 6.1–7.0 ppm was observed. The assignment of this low-field line to hydroxyl protons located at Al–O–Si–O–Al arrangements [26] or at the outer surface of the zeolite particles [76], to bridging hydroxyl protons in weak hydrogen bonds to neighbouring framework oxygen [75], or to mobile hydroxyl protons in dipolar interaction with framework aluminium atoms [77] is still unconfirmed. Further studies are needed to clarify the role of these hydroxyl protons in reactions catalysed by zeolite HZSM-5.

3. Mobility of hydroxyl protons in H-forms of zeolites

The hydroxyl protons of bridging OH groups are not fixed at the zeolite framework [18]. If the mean residence time τ_c of hydroxyl protons is of the same order of magnitude as the inverse of the MAS frequency ($\tau_{rot} = 1/\nu_{rot}$), thermal motion influences the ^{1}H MAS pattern. Assuming a heteronuclear dipole–dipole interaction of hydroxyl protons, described by the second moment [129] M_2^{IS} undergoing uncorrelated statistical jumps, the envelope of the free induction decay is given by [26,144,145]:

$$G(t) = \exp\left\{ -\frac{M_2^{IS}}{3}\left[2J(2\nu_{rot}, t) + J(4\nu_{rot}, t)\right]\right\} \tag{3}$$

with

$$\begin{aligned} J(2\nu_{rot}, t) &= \frac{t\cdot\tau_c}{1+(2\pi\cdot\nu_{rot}\cdot\tau_c)^2} + \frac{\tau_c^2\left(4\pi^2\cdot\nu_{rot}^2\cdot\tau_c^2-1\right)}{\left(1+4\pi^2\cdot\nu_{rot}^2\cdot\tau_c^2\right)^2} \\ &\quad\times\left[1-\exp(-t/\tau_c)\cos(2\nu_{rot}t)\right] \\ &\quad-\frac{4\pi\cdot\nu_{rot}\cdot\tau_c^3}{\left(1+4\pi^2\cdot\nu_{rot}^2\cdot\tau_c^2\right)^2} \\ &\quad\times\exp(-t/\tau_c)\sin(2\nu_{rot}t) \end{aligned} \tag{4}$$

Using $4\nu_{rot}$ instead of $2\nu_{rot}$, the expression for $J(4\nu_{rot}$, it) corresponds to that given in Eq. (4).

Eq. (3) includes several cases which have been discussed in the literature. For the static sample, i.e. for $\nu_{rot} = 0$, Eq. (3) can be transformed as:

$$G^{static}(t) = \exp\left\{-M_2^{IS}\left[\tau_c t + \tau_c^2(\exp - t/\tau_c - 1)\right]\right\} \tag{5}$$

which corresponds to the model of Anderson and Weiss [146]. For MAS ($\nu_{rot} \neq 0$) and a correlation time $\tau_c \gg t$, i.e. the rigid lattice, Eq. (3) becomes

$$\begin{aligned} G^{MAS}(t) &= \exp\left(-\frac{M_2^{IS}}{4\pi^2\cdot\nu_{rot}^2}\left\{\frac{2}{3}\left[1-\cos(2\nu_{rot}t)\right]\right.\right. \\ &\quad\left.\left.+\frac{1}{12}\left[1-\cos(4\nu_{rot}t)\right]\right\}\right) \end{aligned} \tag{6}$$

which corresponds to the expression given by Schneider et al. [147]. If only the envelope of the free induction decay is considered, Eq. (3) becomes

$$G^{\mathrm{MAS}}(t) = \exp\left\{-\frac{M_2^{\mathrm{IS}}t}{3}\left[\frac{2\tau_c}{1+(2\pi\cdot\nu_{\mathrm{rot}}\cdot\tau_c)^2} + \frac{\tau_c}{1+(4\pi\cdot\nu_{\mathrm{rot}}\cdot\tau_c)^2}\right]\right\} \quad (7)$$

Fourier transformation of Eq. (7) yields an expression, first given by Andrew and Jasinski [148], which describes the width of the MAS central line as a function of the correlation time τ_c.

Fig. 6 shows the ^{1}H MAS spectra of hydroxyl protons calculated using Eq. (3) and assuming a heteronuclear dipole–dipole interaction corresponding to a second moment M_2^{HAl} of 4.5×10^8 s^{-2} (SiOHAl group), a MAS frequency ν_{rot} of 3 kHz and correlation times τ_c in the range between 10 ms and 10 μs. While for $\tau_c = 10$ ms (solid) the MAS sideband pattern consists of sharp lines, for correlation times of the order of $\tau_{\mathrm{rot}} = 1/\nu_{\mathrm{rot}}$ the lines become significantly broader. This effect is accompanied by the disappearance of the MAS sidebands. Only for $\tau_c \ll \tau_{\mathrm{rot}}$ does a narrowing occur, and this corresponds to an averaging of the solid-state interaction by isotropic reorientations (mobile). Fig. 7 shows the ^{1}H MAS spectra of dehydrated (673 K) zeolite HZSM-5 (Si/Al = 18) recorded at 293 and 423 K. During the measurement the sample was exposed to nitrogen gas. At 293 K a MAS sideband pattern of SiOHAl at 4.3 ppm and a sharp line of SiOH groups at 2 ppm were observed. At 423 K there is

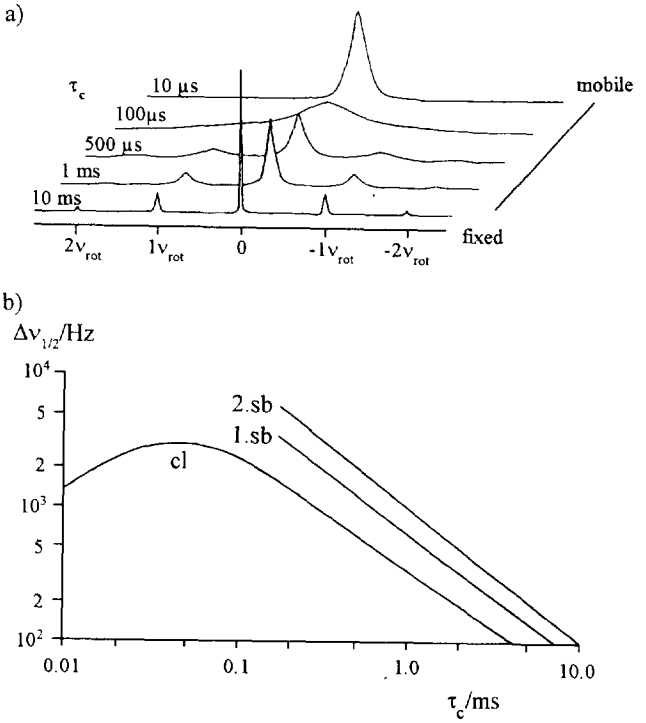


Fig. 6. ^{1}H MAS spectra of hydroxyl protons calculated using Eq. (3) and assuming a heteronuclear dipole–dipole interaction corresponding to a second moment M_2^{HAl} of 4.5×10^8 s^{-2}, a MAS frequency ν_{rot} of 3 kHz and the thermal mobility correlation times τ_c given on the left-hand side of the spectra [26].

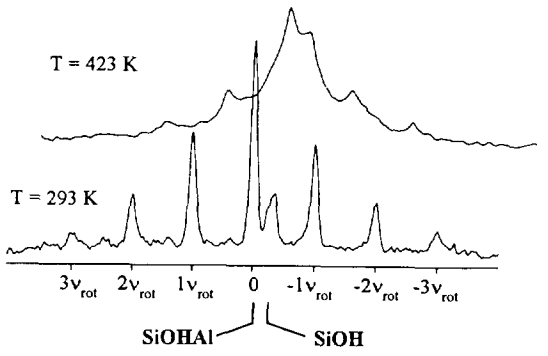


Fig. 7. ^{1}H MAS spectra of zeolite HZSM-5 (Si/Al = 18) dehydrated at 673 K recorded at 400.13 MHz, a MAS frequency ν_{rot} of 3 kHz and at 293 K (bottom) and 423 K (top) [151].

a significant broadening of the MAS sideband pattern of SiOHAl groups, but there is no resonance shift. The fit of the experimental spectrum recorded at 423 K using calculated spectra (Eq. (3)) yielded a correlation time for the hydroxyl protons of the bridging OH groups of about 250 μs [151].

4. Interaction of hydroxyl protons with probe molecules

4.1. Studies of acid–base interactions

Adsorption of probe molecules at dehydrated zeolites is used to characterize the acid strength of OH groups in terms of acid–base interactions. The accessibility of hydroxyl protons to adsorbed probe molecules is considered in Section 4. In the first solid-state ^{1}H studies of dehydrated zeolite HNaY and H-mordenite [17], perdeuterated pyridine was used as the probe molecule. As C_5ND_5 shows no or only weak H–D exchange with acidic hydroxyl protons, only low-intensity lines originating from ring protons overlap the ^{1}H MAS spectrum of dehydrated zeolites. In the ^{1}H MAS spectra of organic acids dissolved in pyridine, lines were observed in the 12–20 ppm range [78]. These lines indicate the formation of the pyridinium ion ($PyrH^+$). Adsorption of pyridine at zeolite HZSM-5 synthesized with tetrapropylamminium ions (TPA^+) [55] produces a shift in the line of SiOH groups from about 1.8 to 9.5 ppm due to the formation of hydrogen bonds with the

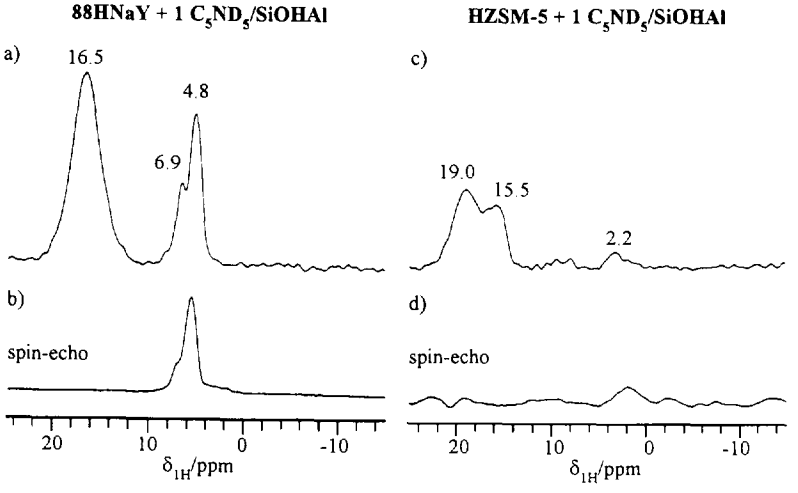


Fig. 8. ^{1}H MAS spectra of dehydrated (673 K) zeolites 88HNaY (a, b) and HZSM-5 (c, d) loaded with one molecule perdeuterated pyridine per bridging OH group, recorded at 400.13 MHz with a MAS frequency ν_{rot} of 10 kHz [79]. (a, c) Spectra recorded with one-pulse excitation; (b, d) spectra recorded using a rotation synchronized Hahn-echo sequence with a pulse delay of 200 μs.

probe molecules, which corresponds to a low acid strength of these hydroxyl protons. The loading of pyridine at acidic zeolites, e.g. HNaHY [36] and HZSM-5 [35,55], gives lines at chemical shifts in the range 15.5–19.5 ppm (Figs. 8(a) and 8(c)). These low-field lines result from a proton transfer to the probe molecules forming the pyridinium ions. At the same time, the lines of the acidic bridging OH groups which are involved in this proton transfer disappear. In ^{1}H MAS spectra recorded using a spin–echo $\pi/2-\tau-\pi-\tau$ sequence with pulse delays τ which are multiples of the MAS period, exclusive lines of rigid hydroxyl protons or complexes were refocused in the Hahn echoes [34,52,79]. The ^{1}H MAS spectra shown in Figs. 8(b) and 8(d) were recorded using this technique. By contrast to the spectra in Figs. 8(a) and 8(c), those in Figs. 8(b) and 8(d) show no low-field lines from the pyridinium ions which indicates a high mobility of $PyrH^+$ in zeolites 88HNaY and HZSM-5 at room temperature. This suggestion is supported by variable-temperature ^{1}H MAS experiments. Fig. 9 shows the ^{1}H MAS spectra of zeolite 88HNaY loaded with pyridine and recorded at 223–423 K using one-pulse excitation. The strong increase in the MAS sideband pattern from the $PyrH^+$ line (marked by asterisks) occuring at $T \leq 273$ K indicates a reduced mobility of $PyrH^+$. No further significant change in this pattern was observed at temperatures down to 123 K. However, the disappearance of this MAS sideband pattern at above 323 K points to an increasing mobility of $PyrH^+$ complexes in this temperature range. In addition, it is interesting to note the decrease in the line intensity of bridging OH groups located in the sodalite cages (4.8 ppm) at $T \geq 323$ K. As there is no change in the line intensity of ring protons at 6.9 ppm, the former effect is explained by a migration of hydroxyl protons from the sodalite cages into the supercages, where they are involved in the protonation of pyridine molecules.

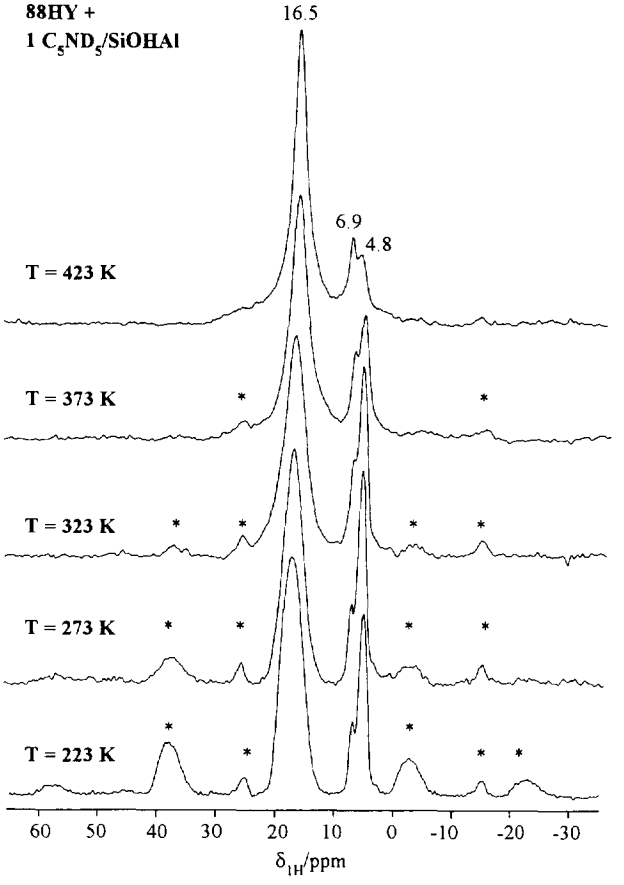


Fig. 9. ^{1}H MAS spectra of dehydrated (673 K) zeolite 88HNaY loaded with one molecule deuterated pyridine per bridging OH group, recorded at 400.13 MHz, a MAS frequency ν_{rot} of 8 kHz and 223–423 K [151].

Ammonia has been used as a probe molecule in a number of ^{1}H MAS studies of acidic zeolites [18,31,35,36,80–83]. As the H-forms of zeolites are often prepared by cation exchange in an aqueous solution of NH_4NO_3 and subsequent calcination, weak ^{1}H MAS lines in the range 6.8–7.4 ppm indicate the existence of residual ammonium ions [18,67,71]. Adsorption of ammonia on dehydrated H-zeolites leads to the formation of ammonium ions which produce a ^{1}H line at the same resonance position as discussed above [35,81]. At adsorbed molecule/acidic bridging OH group ratios of $n < 1$, the adsorption of ammonia molecules causes a decrease in the line of bridging OH groups while the lines of ammonium ions (at about 7 ppm) increase (Fig. 10(a)). The decrease in the line at 3.9 ppm found for low loadings indicates a favoured ammmoniation of the bridging OH groups in the supercages of zeolite HNaY. At $n = 1$, corresponding to one equivalent of probe molecules per bridging OH

group, the ^{1}H MAS spectrum consists exclusively of lines from ammonium ions at 6.8 and 7.4 ppm (Fig. 10(b)). For $n > 1$ a high-field shift of the main line occurs, which originates from a rapid exchange of ammonium ions (at about 7 ppm) and physisorbed ammonia molecules (at about 3.2 ppm) [35,81]. Two weak lines at 6.8 and 5.3 ppm which do not undergo the high-field shift were attributed to single ammonium ions and NH_3–NH_4^+ complexes, respectively, in the sodalite cages [35,81]. The fixed resonance positions of these lines indicate that on the NMR time-scale single ammonium ions as well as the NH_3–NH_4^+ complexes in the sodalite cages do not undergo rapid exchange with free ammonia molecules in the supercages. No restriction of the ammonia mobility has been observed in ^{1}H MAS studies of zeolite HZSM-5 [35,81] and silicoaluminophosphates SAPO-5 (structure type AFI) and SAPO-34 (structure type CHA) [80].

Dehydrated zeolites HCsNaY and HNaY loaded with ammonia were studied by Jacobs et al. [82]. Zeolite HCsNaY (35 Cs^+/u.c.) was prepared by a successive exchange in aqueous solutions of NH_4NO_3 and CsCl. The results for zeolites HNaY (Si/Al between 2.4 and 12.0) agree well with those described above [35,81]. However, adsorption of ammonia on zeolite HCsNaY produced a low-field ^{1}H MAS line at 8.1 ppm. The line at about 7 ppm is split into two components, one at 6.5 ppm and the other at 6.9 ppm. The authors [82] attributed the line at 6.9 ppm to ammonium ions in the supercages and the lines at 6.5 and 8.1 ppm to ammonium ions in the sodalite cages at cationic positions SII′ and SI′ (Fig. 1), respectively. Excluding the possible influence of cesium cations on the chemical shift of the ammonium ions, this assignment was used for the interpretation of ^{1}H MAS spectra of zeolites HCsNaY and HNaY. However, as no line from ammonium ions was observed at 8.1 ppm for zeolites HY in previous studies (see above), its appearance in zeolite CsNaY must be considered to be associated with the presence of cesium cations. The two ^{1}H lines at about 7 ppm can be explained by the presence ammonium ions at different positions or in different cages. The favoured ammoniation of bridging OH groups in supercages (Fig. 10(a)) and the intensity ratio of 2:1 observed for the lines at 6.8 and 7.4 ppm in

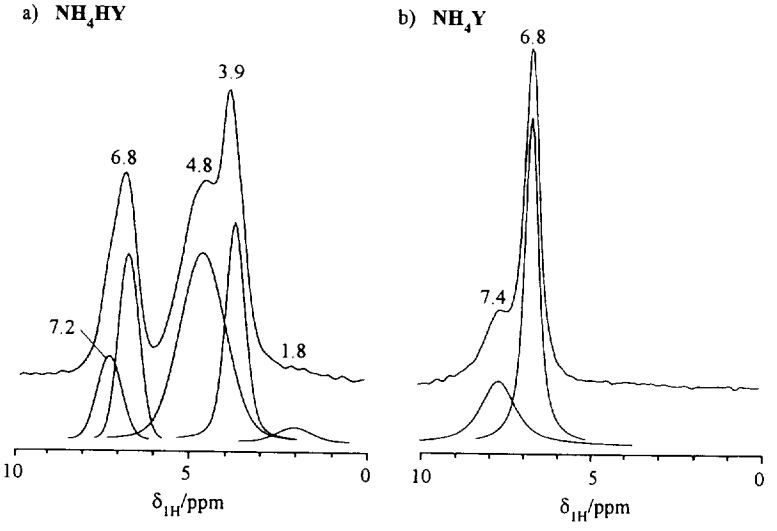


Fig. 10. ^{1}H MAS spectra of dehydrated (673 K) zeolite 88HNaY loaded with about 5 (a) and 48 (b) molecules of ammonia per unit cell, recorded at 400.13 MHz and a MAS frequency ν_{rot} of 10 kHz [151].

Fig. 10(b) (lines at 6.5 and 6.9 ppm in Ref. [82]) indicate that these lines originate from ammonium ions in the supercages and the sodalite cages, respectively.

Variable-temperature ^{1}H MAS NMR studies of hydroxyl protons in zeolite HZSM-5 interacting with probe molecules via hydrogen bonds have been reported by White et al. [84]. To study the slow-exchange range in the presence of adsorbed molecules, the authors carried out low-temperature MAS measurements. The probe molecules used were acetylene, ethylene, carbon monoxide, benzene, ethane and nitrogen. After adsorption of 3.0 equivalents of acetylene per acidic OH group, a low-field shift of the ^{1}H resonance position of the bridging OH groups from 4.3 to 7.3 ppm was observed at 298 K (Fig. 9(a)). This corresponds to an observed low-field shift of $\Delta\delta_{obs} = 3.0$ ppm. After adsorption of 0.9 equivalents of acetonitrile, Haw et al. [85] found a resonance shift of the bridging OH groups in zeolite HZSM-5 from 4.3 to 11.5 ppm. Loading of about 1 equivalent of ethylene, carbon monoxide and ethane caused an observed low-field shift of up to 2.0, 1.5 and 0.3 ppm, respectively [84]. At 123 K an adsorbate-induced low-field shift of 2.7 ppm for ethylene, 1.8 ppm for carbon monoxide and 0.6 ppm for ethane. Hence, the adsorbate-induced low-field shift of hydroxyl protons is extremely sensitive to the type of probe molecule. The observed loading-dependent low-field shifts of acetylene and carbon monoxide at 298 K (Fig. 11(b)) suggest an exchange, averaging the lines of the free bridging OH groups and the bridging OH groups which are associated via hydrogen bonds with the probe molecules. At 123 K and adsorption of less than 1.0 equivalent of probe molecule, the ^{1}H MAS lines of free and bonded hydroxyl protons were clearly resolved (Fig. 11(a)).

The ^{1}H low-field shift as a function of temperature of the bridging OH groups in zeolite HZSM-5 after the adsorption of about 1 equivalent of carbon monoxide was studied by Koch et al. [86]. At 123 K the authors found a low-field shift of the resonance position of bridging OH groups from 4.2 to 6.2 ppm, which corresponds to $\Delta\delta_{obs} = 2.0$ ppm. The adsorbate-induced wavenumber shift in the IR stretching vibrations of bridging OH groups was $\Delta\nu = 300$ cm^{-1}. Considering the linear correlation of the IR wavenumbers and ^{1}H MAS shifts of hydrogen-bonded hydroxyl protons [47], from this IR wavenumber shift a low-field NMR shift of $\Delta\delta_{1H} = 2.8$ ppm was estimated [86]. This indicates that even at 123 K the influence of thermal motion on the ^{1}H resonance position of the adsorbate complex is not completely removed. From a quantitative analysis of the ^{1}H MAS intensities, Brunner

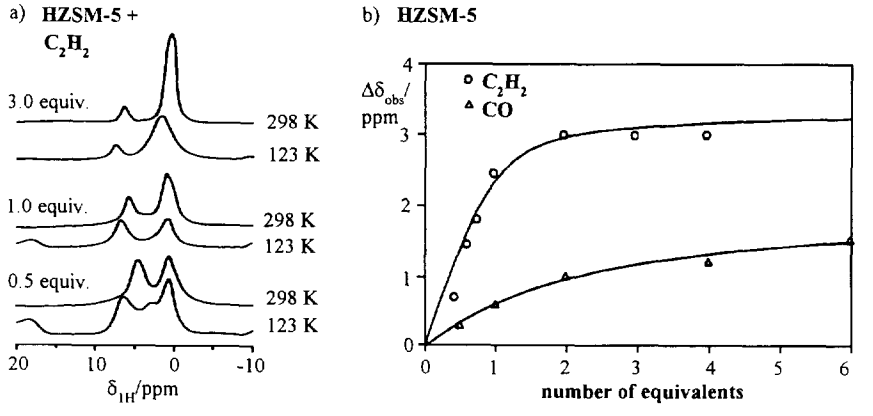


Fig. 11. (a) ^{1}H MAS spectra of dehydrated (673 K) zeolite HZSM-5 (Si/Al = 38) loaded with various equivalents of acetylene, recorded at 299.7 MHz, a MAS frequency ν_{rot} of about 6 kHz and at 298–123 K (taken from Ref. [84]). (b) The observed low-field shifts, $\Delta\delta_{obs}$ of the ^{1}H resonance positions of the hydroxyl protons in zeolite HZSM-5 loaded with acetylene and carbon monoxide, measured at 298 K.

et al. [87] concluded that the low-field shifted line at 6.2 ppm is caused by free bridging OH groups at 4.2 ppm in the spectrum of unloaded zeolite HZSM-5 as well as by hydroxyl protons which appear at resonance positions in the 6.1–7.0 ppm range (see Section 2 and last row of Table 2). In view of this result, the authors suggest that the two types of OH group in zeolite HZSM-5 both have the same acid strength.

The ^{15}N cross polarization (CP) MAS NMR of pyridine adsorbed at zeolites [88] is an indirect method of monitoring Brønsted acidity. However, the chemical exchange of pyridine molecules at different adsorption sites with different efficiencies of CP makes quantitative evaluation difficult [89]. The use of trimethylphosphine (TMP) as the probe molecule for the Brønsted sites has the advantage of a high sensitivity and well-resolved ^{31}P MAS spectra. ^{31}P NMR of TMP is therefore used for the characterization of acidic zeolites [90–93] and amorphous catalysts [94,95]. Biaglow et al. [96] have described ^{13}C MAS NMR studies of C2 labelled acetone adsorbed on zeolites HZSM-5, HZSM-12 (structure type MTW), HZSM-22 (structure type TON), HY, H-mordenite, SAPO-5 and MeAPO-5 (structure type AFI) at 125 K. The adsorption of about 1 equivalent of acetone produces a low-field shift of the resonance position of C2 atoms relative to the neat solid in the range between 10.1 ppm for SAPO-5 and 18.7 ppm for HZSM-22. The authors suggest that the ^{13}C NMR shift of carbonyl carbon atoms in acetone may be used as a measure of the intrinsic acid strength of the Brønsted sites in zeolites.

4.2. Complex formation and protonation equilibrium

Loading-dependent resonance shifts of the ^{1}H lines of bridging OH groups (Fig. 11(b)) are a function of the equilibrium constant K:

$$K = \frac{[\mathrm{ZOH - ADS}]}{[\mathrm{ADS}][\mathrm{ZOH}]} \tag{8}$$

where [ZOH–ADS], [ADS] and [ZOH] are the equilibrium concentrations of adsorption complexes, free adsorbate molecules and free acidic hydroxyl protons, respectively, related to the total concentration of hydroxyl protons. The equilibrium constants K of the formation of hydrogen bonded complexes which consist of acidic hydroxyl protons and acetylene or carbon monoxide were determined by White et al. [84] using the low-field shifts $\Delta\delta_{obs}$ shown in Fig. 11(b). As at 298 K the adsorbate molecules are in fast exchange, the observed low-field shift is a function of the maximum low-field shift $\Delta\delta_{max}$ given by the low-field shift of hydroxyl protons in the slow-exchange limit at low temperatures. With the equilibrium constant K and the whole concentration of adsorbate molecules $C_{ads} = [\mathrm{ADS}]$

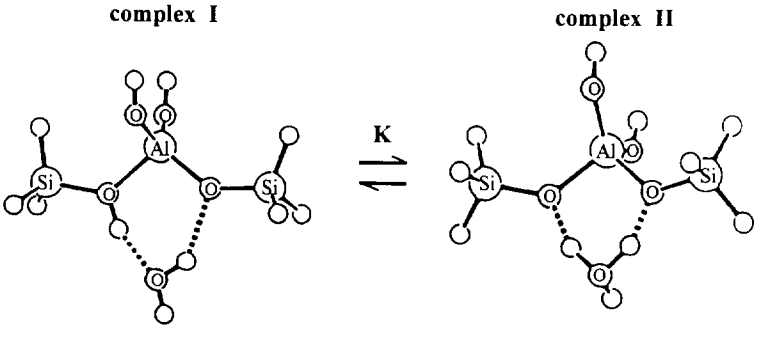


Fig. 12. Adsorbate complexes of water molecules interacting with model clusters of bridging OH groups derived by quantum-chemical calculations (taken from Ref. [97]). Complex I shows the physisorption of a water molecule via two hydrogen bonds; complex II shows a hydrogen bonded hydroxonium ion.

+ [ZOH–ADS], the observed low-field shift becomes [84]:

$$\Delta\delta_{obs} = \Delta\delta_{max}\frac{\left(1+C_{ads}+\frac{1}{K}\right)-\sqrt{\left(1+C_{ads}+\frac{1}{K}\right)^2-4C_{ads}}}{2} \quad (9)$$

The curves shown in Fig. 11(b) were calculated using the maximum shift values of 3.3 and 1.8 ppm [84] determined from the ^{1}H shifts of acidic hydroxyl protons in zeolite HZSM-5 loaded with acetylene and carbon monoxide, respectively, at 123 K. The smooth curves, which are in excellent agreement with the experimentally observed values, yielded equilibrium constants K of 7.0 and 0.7 per equivalent, respectively. The difference in the constants reflects the different strengths of the hydrogen bonds formed by the interaction of acetylene and carbon monoxide with the acidic OH groups in HZSM-5.

Using water as a probe to study the acidic strength of Brønsted centres in zeolites has several advantages. Water molecules are small enough to gain access to OH groups in the supercages and channels as well as those in small cavities and six-membered oxygen rings. In addition, water has a convenient basic strength and hardness which allows the equilibrium between the hydrogen-bonded and protonated complexes I and II (Fig. 12) to be investigated. Complex II corresponds to the formation of hydroxonium ions (H_3O^+). The geometries of complexes I and II were determined by using quantum chemical methods [97,98]. The affinity of water molecules to sorption centres in zeolites was calculated by Sauer and co-workers [99,100] as 791 kJ mol^{-1} for H_2O at Al^{3+}, 117 kJ mol^{-1} at Na^+, 58 kJ mol^{-1} at SiOHAl, 20 kJ mol^{-1} for bulk H_2O and 16 kJ mol^{-1} for H_2O at SiOH. Therefore, the hydration of zeolites starts with the adsorption of water molecules at Lewis sites and cationic species, followed by adsorption at bridging OH groups. However, in H-zeolites not containing extra-framework aluminium, bridging OH groups are the favoured sorption centres. In a number of investigations [53,101–105] wide-line ^{1}H at 4 K was successfully applied to study frozen adsorbate complexes formed by the adsorption of water on solid acids. For water adsorbed on H-zeolites, the ^{1}H lines from the following species must be taken into account: (a) free hydroxyl protons of bridging OH groups (n_{OH}); (b) free water molecules (n_{H_2O}); (c) water molecules physisorbed at bridging OH groups via hydrogen bonds (n_{OH-OH_2} complexes I); and (d) hydroxonium ions ($n_{H_3O^+}$ complexes II). Deconvolution of the wide-line ^{1}H spectrum recorded at 4 K allows the concentrations of these species to be determined. Thus deconvolution of the spectrum of zeolite HY (Si/Al = 2.42) loaded with 1 equivalent of water molecules has shown that the values of n_{OH} and n_{H_2O} are negligibly small [103,104]. Therefore, the equilibrium constant K for the formation of hydroxonium ions is given exclusively by the numbers of complexes I and II. For zeolite HY loaded with 1 equivalent of water molecules, Batamack et al. [103,104] found $n_{H_3O^+} = 9.7 \pm 2.0$ u.c.$^{-1}$ and $n_{OH-OH_2} = 38.6 \pm 2.0$ u.c.$^{-1}$, corresponding to an equilibrium constant K of $n_{H_3O^+}/n_{OH-OH_2} = 0.25 \pm 0.05$. These authors proposed a scale of the acid strength of Brønsted sites in solid acids [104] given by the ratio of $n_{H_3O^+}$ (determined after adsorption of 1 equivalent of water molecules) and n_{OHa} of the initially observed acidic OH groups. The value of this ionization coefficient is zero for silanol groups, 0.2 for bridging OH groups in zeolite HY, 0.4 for hydroxyl protons in $H_2Sb_4O_{11} \cdot 2H_2O$ and 1.0 for sulphonic acid groups in Nafion-H (perfluorinated resinsulphonic acid).

Fast chemical exchange between complexes I and II at room temperature results in only one ^{1}H line for all species [52,53,106]. Consequently, the adsorption of a small amount of water (20 H_2O/u.c.) on zeolite HNaY (Si/Al = 2.6) with 46 ± 4 SiOHAl/u.c. dehydrated at 673 K causes the ^{1}H MAS sideband pattern to disappear [52]. With increasing amounts of adsorbed water, the centre of gravity of the ^{1}H line undergoes a low-field shift. After the adsorption of about 1 equivalent of water, the centre of gravity is at $\delta_{cg} = 6.2$ ppm [52]. Considering the results from wide-line ^{1}H, this line is caused exclusively by protons contributing to complexes I and II (Fig. 12). Therefore, the resonance position of the centre of gravity can be calculated as the weighted

average of the chemical shifts δ_I and δ_{II}:

$$\delta_{cg} = (1-p)\delta_I + p\delta_{II} \quad (10)$$

Conversely, if the mean chemical shifts δ_I and δ_{II} of the protons in complexes I and II, respectively, are known, the fractions p and $(1-p)$ of these complexes can be estimated. Complex I consists of (a) one hydroxyl proton of the bridging OH group hydrogen-bonded to the water molecule, (b) one hydroxyl proton of the water molecule hydrogen bonded to the zeolite framework and (c) one free hydroxyl proton at the water molecule. The chemical shift of an isolated water molecule in the gaseous phase amounts to $\delta_c = 0.3$ ppm [107]. The chemical shift of bulk water [108] can be used as the value ($\delta_b = 4.8$ ppm) for hydrogen-bonded water protons. The addition of the low-field shift of about 4.5 ppm, due to the hydrogen bonding of water protons to neighbouring water molecules, and the chemical shift of free bridging OH groups in zeolite HY of 3.9 ppm, leads to the value of $\delta_a = 8.4$ ppm. Finally, the arithmetic average of δ_a, δ_b and δ_c yields a value of $\delta_I = 4.5$ ppm, which corresponds to the mean ^{1}H shift of complex I. For two-fold hydrogen-bonded hydroxonium ions (complex II) a mean ^{1}H shift of about $\delta_{II} = 13$ ppm was estimated [52,53]. Using Eq. (10) and the experimental value of $\delta_{cg} = 6.2$ ppm, the fraction of protons contributing to complex II is $p = 0.2$. At room temperature, therefore, the formation of hydroxonium ions is characterized by the equilibrium constant $K = p/(1-p) = 0.25$, which is in excellent agreement with the equilibrium constant determined by wide-line ^{1}H NMR for the system at 4 K (see above). For zeolite HZSM-5 (Si/Al = 20) loaded with 1 equivalent of water, a value of $\delta_{cg} = 7.7$ ppm was measured [149], corresponding to $K = 0.6$. The different values of K (0.25 for zeolite HY and 0.6 for HZSM-5) can be explained in terms of the mean framework electronegativities S^m (see Table 1 and Fig. 3) of these zeolites. The lower framework aluminium content of zeolite HZSM-5 corresponds to a higher value of S^m and, therefore, to a higher acid strength of the Brønsted centres. Hence, the equilibrium in the protonation reaction is shifted towards the hydroxonium ions.

4.3. Chemical status of hydroxyl protons interacting with probe molecules

The transformation of alcohols to higher hydrocarbons over zeolites is the basis of several reactions developed for applications in industrial processes, such as MTG (methanol to gasoline) [109,110]. A number of recent quantum chemical studies [7,13,15,16] have been done with the aim of finding a theoretical description of the complexes formed by the adsorption of methanol molecules at bridging OH groups. These studies suggest that physisorption of methanol at cluster

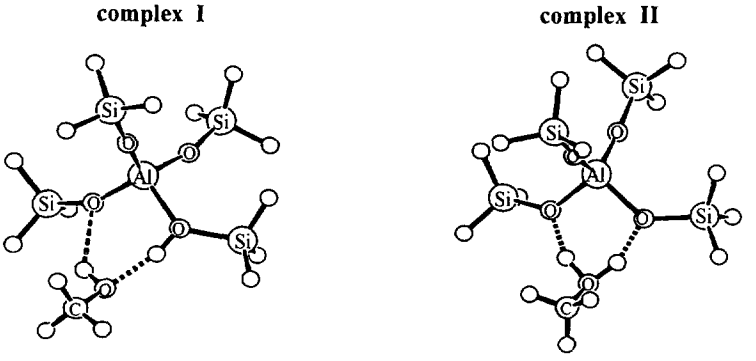


Fig. 13. Adsorbate complexes of methanol molecules interacting with the model clusters of bridging OH groups derived by quantum-chemical calculations (taken from Ref. [13]). In complex I a methanol molecule is physisorbed via two hydrogen bonds while in complex II a methoxonium ion is hydrogen bonded at the cluster.

models of bridging OH groups via two hydrogen bonds (complex I, Fig. 13) is the most stable binding geometry, while a methoxonium cation complexed to the deprotonated fragments (complex II, Fig. 13) was found to be a transition state and not a local minimum. Sauer and co-workers [7,13,15] concluded that proton transfer from the aluminosilicate cluster is favourable with a heat of reaction of about 12 kJ mol^{-1}. In addition, a mean ^{1}H shift of about 5.7 ppm was calculated [13] for the neutral hydrogen-bonded complex I and of 15.3 ppm for the ion-pair complex II.

The first multinuclear solid-state NMR studies of methanol adsorbed at zeolites were carried out by Luz and Vega [111] who studied the interaction of methanol molecules and the hydroxyl protons of SiOHAl groups in zeolites HRHO and HY by ^{1}H, ^{27}Al and ^{29}Si MAS NMR. ^{27}Al and ^{29}Si MAS indicate that the adsorption behaviour of water and methanol is similar. Adsorption of either causes a narrowing of the lines from framework aluminium and silicon atoms, indicating a relaxation of the symmetry of the zeolitic framework. In the ^{1}H MAS spectra a methanol-induced shift of the hydroxyl protons of the bridging OH groups in zeolite HRHO from 3.7 ppm to a maximum of 10.5 ppm was observed. High coverages of methanol at zeolite HZSM-5 were studied by ^{1}H MAS NMR [112–115]. According to Anderson et al. [114], saturation of zeolites with CD_3OH shifts the line from hydroxyl protons to 9.4 ppm in zeolite HZSM-5, 5.6 ppm in SAPO-34, 5.2 ppm in HL (structure type LTL) and SAPO-5, 5.1 ppm in zeolite HY and 4.8 ppm in SAPO-11 (stucture type AEL). Based on the results derived from zeolite HZSM-5 loaded with 6 equivalents of methanol, the formation of formally identical hydrogen bonded and/or direct protonated methanol molecules was suggested [112–114]. However, the high coverage of zeolite HZSM-5 by probe molecules should cause a rapid exchange between free and bonded molecules and/or between different adsorbate structures. Therefore, neither the shift values nor the fact that only one resonance position is observed provides a decisive argument for an identical chemi-

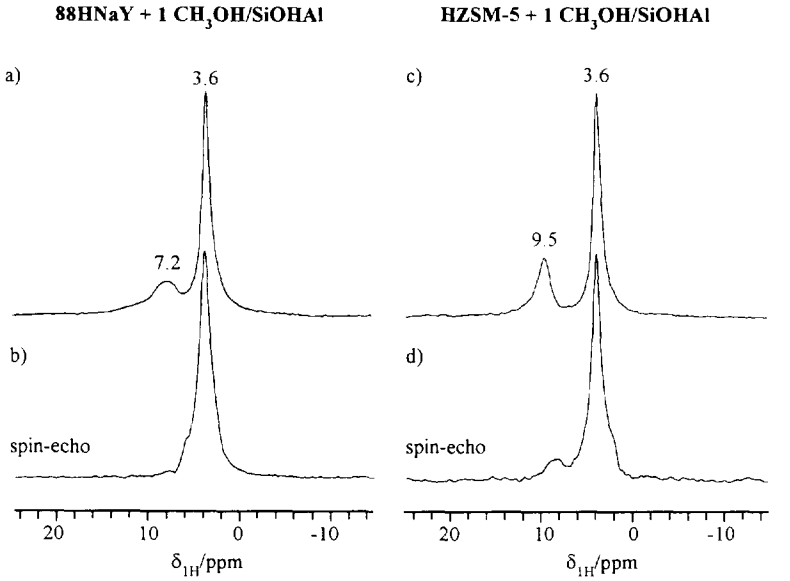


Fig. 14. ^{1}H MAS spectra of dehydrated (673 K) zeolites 88HNaY (a, b) and HZSM-5 (c, d) loaded with one molecule of methanol per bridging OH group and measured at 400.13 MHz with a MAS frequency ν_{rot} of 10 kHz [79]. (a, c) Spectra were recorded with one-pulse excitation; (b, d) spectra recorded using a rotation-synchronized Hahn-echo sequence with a pulse delay of 1.2 ms.

cal interaction of the methanol molecules within a cluster or for the formation of complexes I or II.

Recent multinuclear solid-state NMR studies of methanol adsorbed on zeolites 88HY (Si/Al = 2.6) and HZSM-5 (Si/Al = 22.0) dehydrated at 673 K [79] have shown that after adsorption of methanol the ^{1}H MAS spectra consist of lines at 3.6 and 7.2 ppm for zeolite 88HNaY (Fig. 14(a)) and at 3.6 and 9.5 ppm for zeolite HZSM-5 (Fig. 14(c)). While the line at 3.6 ppm comes from the CH_3 groups of methanol, the lines at 7.2 and 9.5 ppm were assigned to hydroxyl protons involved in the interaction between zeolitic OH groups and methanol molecules. In the spectra of zeolites 88HNaY and HZSM-5 loaded with up to 3 equivalents of methanol, low-field resonance shifts of the hydroxyl protons were observed which agree with those reported by Anderson et al. [114]. The spectra shown in Figs. 14(b) and 14(d) were recorded using a rotation-synchronized spin-echo sequence in order to study the mobility of hydroxyl protons and adsorbate complexes (see Fig. 8). In the ^{1}H MAS spectra recorded with a pulse delay of 1.2 ms, the lines at 7.2 ppm (88HNaY) and 9.5 ppm (HZSM-5) disappear, but a shoulder at 5.8 ppm for zeolite 88HNaY (Fig. 14(b)) and a line at 8.5 ppm are observed for zeolite HZSM-5 (Fig. 14(d)). This indicates that the low-field lines of hydroxyl protons in the ^{1}H MAS spectra of zeolites loaded with 1 equivalent of methanol consist of lines from mobile hydroxyl protons involved in a rapid exchange between a component with a high chemical shift, probably methoxonium ions (complex II), and a component with a lower chemical shift, possibly hydroxyl protons forming hydrogen bonds with methanol (complex I).

Protonation and deprotonation of the Si–O–Al bridges and their influence on the NMR parameters of the T atoms have been studied by ^{29}Si MAS and static ^{27}Al NMR [43,79] using dehydrated samples loaded with benzene, ammonia, pyridine and methanol. ^{29}Si MAS demonstrated that deammoniation of zeolite HZSM-5 produces a shift of the Si(1Al) line from −104.8 to −107.5 ppm, corresponding to a change in the mean Si–O–T bond angle of 3.5–5° [43,79]. No change in the ^{29}Si resonance position was observed after deammoniation of zeolite 88HNaY and after adsorption of 1 equivalent of benzene, pyridine or methanol on dehydrated 88HNaY and HZSM-5. The ^{27}Al spectra of dehydrated 88HNaY and HZSM-5, recorded with a quadrupole-echo sequence [19,143], contain two types of line: (i) a narrow line (QL) of framework aluminium atoms

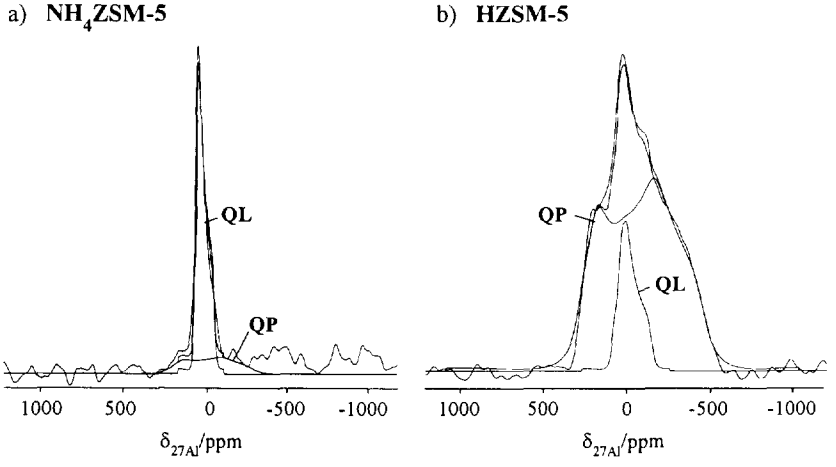


Fig. 15. Deconvolution of the ^{27}Al NMR spectra of zeolites NH_4ZSM-5 (a) and HZSM-5 (b) dehydrated at 433 and 673 K [151], respectively, and recorded at 104.3 MHz using the quadrupole-echo sequence described in Ref. [143].

with a quadrupole coupling constant (QCC) of 5.0–7.5 MHz; and (ii) a broad quadrupolar pattern (QP) corresponding to a QCC of 13.0–16.0 MHz (Fig. 15). Table 3 summarizes the ^{27}Al NMR parameters derived from unloaded and loaded zeolites Y and ZSM-5. Line QL dominates the spectra of dehydrated zeolites Y and ZSM-5 containing cationic species, e.g. Na^+ [19], NH_4^+ (Fig. 15(a)), pyridinium ions (Fig. 16(c)) and adsorbed methanol (Fig. 16(c)). However, after deammoniation (i.e. after the formation of SiOHAl groups) the spectra of dehydrated 88HNaY and HZSM-5 (Fig. 16(a)) are dominated by line QP. Protonation of the Si–O–Al bridge causes a significant change in the charge distribution within the AlO_4 tetrahedra and thus an increase in the quadrupole coupling constant of framework aluminium. Upon adsorption of benzene the hydroxyl protons of the SiOHAl groups form weak hydrogen bonds, but are still located at framework oxygen atoms, and therefore the ^{27}Al spectra show the same features as those of unloaded 88HNaY and HZSM-5 (Fig. 16(b)). By contrast, after adsorption of methanol on dehydrated 88HNaY and

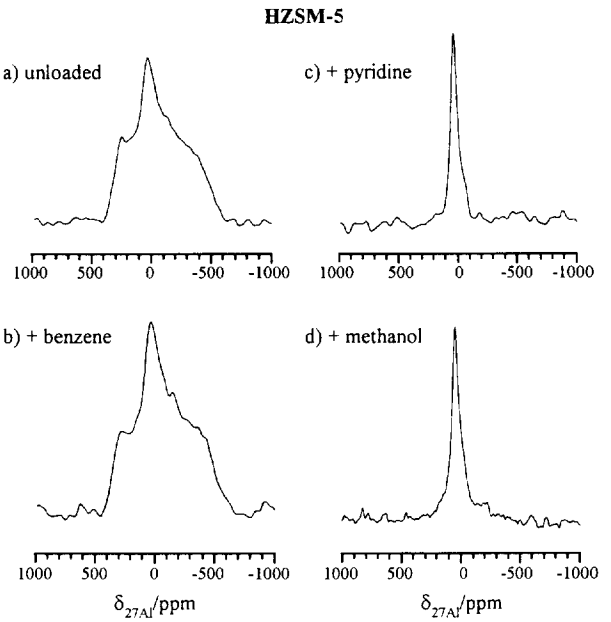


Fig. 16. ^{27}Al NMR spectra of dehydrated (673 K) zeolite HZSM-5 unloaded (a) and loaded with 1 equivalent of benzene (b), pyridine (c) and methanol (d) [79]. The spectra were recorded at 104.3 MHz using the quadrupole-echo sequence described in Ref. [143].

Table 3
Quadrupole coupling constant (QCC), asymmetry parameter (η_Q) of the electric field gradient, isotropic chemical shifts (δ_{iso}) and relative intensities (I_{rel}) of the ^{27}Al NMR lines (central transition) of framework aluminium atoms in ammonium-exchanged zeolites $88NH_4NaY$ (Si/Al = 2.6) and NH_4ZSM-5 (Si/Al = 22.0) after calcination at 433 K and in zeolites 88HNaY and HZSM-5 dehydrated at 673 K before and after adsorption of 1 equivalent of pyridine, benzene and methanol [43,79] [a]

Sample	QCC (MHz)	η_Q	δ_{iso} (ppm)	I_{rel} (%)
$88NH_4NaY$	5.0	0.65	60	87
	10.7	0.6	55	13
88HNaY	6.0	0.7	55	17
	13.7	0.5	50	83
88HNaY + C_6D_6	5.3	0.7	55	12
	13.3	0.4	50	88
88HNaY + C_5ND_5	4.7	0.7	55	63
	12.0	0.5	50	37
88HNaY + CH_3OH	5.7	0.7	55	79
	12.0	0.45	50	21
NH_4ZSM-5	5.7	0.7	60	81
	10.7	0.6	56	19
HZSM-5	7.3	0.7	55	26
	16.3	0.5	50	73
HZSM-5 + C_6D_6	7.3	0.75	55	22
	15.0	0.4	60	78
HZSM-5 + C_5ND_5	5.2	0.75	55	100
HZSM-5 + CH_3OH	5.2	0.8	55	100

[a] The data were derived from static ^{27}Al NMR spectra recorded at 104.3 MHz using the quadrupole-echo sequence described in Ref. [143].

HZSM-5, the ^{27}Al spectra show a narrow QL line (Fig. 16(d)), which is caused by the deprotonation of AlO_4 tetrahedra contributing to the SiOHAl groups that interact with methanol. Deprotonation of the framework is accompanied by a sharp decrease in the electric field gradient at framework aluminium and, therefore of the QCC. As deprotonation of the framework corresponds to protonation of the probe molecules, the observed changes in the QCC confirm the formation of methoxonium ions. Averaging of the electric field gradient by molecular jumps of methanol molecules can be excluded, because static ^{1}H and ^{27}Al spectra measured at 85 K (Ref. [73]) show a strong decrease in molecular mobility, while no change in the aluminium NMR lineshape is observed. Therefore, ^{1}H and ^{27}Al NMR support the formation of methoxonium ions (complex II) as the dominant mechanism of chemical interaction.

5. Location of hydroxyl protons in zeolites

5.1. Location of hydroxyl protons studied by probe molecules

Adsorption of probe molecules is a convenient method for the examining the location of hydroxyl protons in microporous solids. Mastikhin et al. [33] isolated the ^{1}H MAS lines of hydroxyl protons located at the outer surface and inside the particle of γ-Al_2O_3 and η-Al_2O_3 by H–D exchange with adsorbed D_2O molecules. Adsorption of deuterated cyclohexane (kinetic diameter 0.6 nm [116]) at dehydrated SAPO-5 causes the disappearance of the ^{1}H line at 3.8 ppm from bridging OH groups, which was explained by a H–D exchange between probe molecules and the hydroxyl protons [80]. This indicates that the hydroxyl protons involved are located in 12-ring channels (diameter 0.73 nm [117]). The ^{1}H MAS spectrum recorded 10 days later shows two weak lines at about 3.8 and 4.8 ppm, brought about by slow migration of deuterons and protons between the bridging OD and OH groups in 12-ring channels and six-membered oxygen rings, respectively. However, adsorption of deuterated pyridine (kinetic diameter 0.58 nm [116]) on dehydrated SAPO-5 showed that both types of bridging OH group (at 3.8 and 4.8 ppm) interact with the probe molecules [80]. Hence, adsorption of a strong base on SAPO-5 may cause migration of hydroxyl protons from six-membered oxygen rings into the 12-ring channels. However, after adsorption of pyridine on SAPO-34 there was no change in the line of bridging OH groups at 3.8 ppm [80].

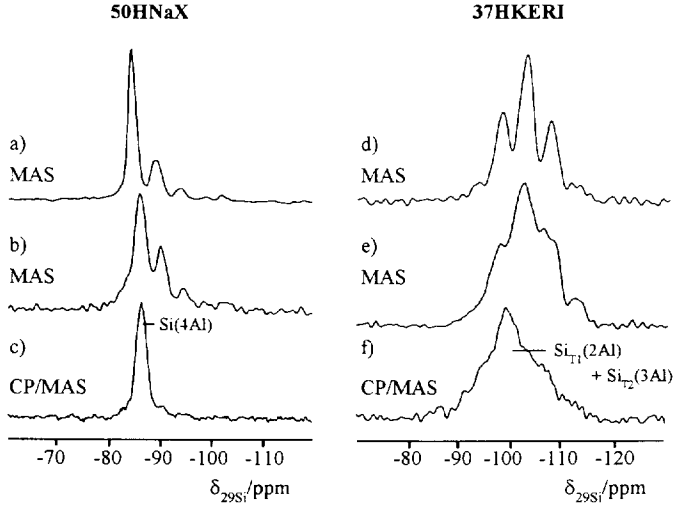


Fig. 17. ^{29}Si MAS spectra of hydrated (a, d) and calcined (b,c,e,f) zeolites 50HNaX (a–c) and 37HKERI (d–f) recorded at 79.5 MHz with a MAS frequency ν_{rot} of 4.5 kHz without (a, b, d, e) and with (c, f) application of cross-polarization using a 3 ms contact time [37].

The probe molecules cannot enter the chabazite cages through the eight-ring windows (diameter 0.38 [117]). However, ammoniation of dehydrated zeolite SAPO-34 produced a ^{1}H MAS line at 6.5 ppm from the ammonium ions [80]. This proves the accessibility of bridging OH groups located in the chabazite cages to molecules comparable in size to ammonia (kinetic diameter 0.26 nm [116]).

5.2. Location of dipolar coupled hydroxyl protons

^{29}Si MAS NMR of hydrated zeolites with cross-polarization (CP) enables one to enhance the lines of the Q^3 (Si(3T,OH)) and Q^2(Si(2T, 2OH) silicon atoms of SiOH groups at about -100 and -90 ppm, respectively [118]. The type of Si(nAl) sites in Si–O–Al bridges forming bridging OH groups were indentified by ^{29}Si CP/MAS NMR of dehydrated zeolites [37], where the rigid location of hydroxyl protons leads to a strong increase in their dipolar interaction with the adjacent silicon atoms. Therefore, application of CP enhances the ^{29}Si MAS lines from Si(nAl) atoms ($n = 4$, 3, 2 or 1) involved in SiO-HAl arrangements [37]. Fig. 17 shows the ^{29}Si MAS spectra zeolites X (Si/Al = 1.4) and erionite (Si/Al = 2.9) after 50% and 37% ammonium ion exchange, respectively, followed by calcination at 673 K. The spectra were recorded without and with CP. In the ^{29}Si CP/MAS spectra of zeolite 50HNaX (Fig. 17(c)) only the Si(4Al) line is enhanced while the Si(3Al) and Si(2Al) lines disappear. In zeolite 37HKERI (Fig. 17(f)), which has two crystallographically inequivalent T1 and T2 sites [117], an enhancement of the Si_{T1}(2Al) + Si_{T2}(3Al) line was found in the ^{29}Si CP/MAS spectra. The Si(nAl) lines of T1 and T2 sites with $n < 2$ and 3, respectively, produce only a broad high-field shoulder. This indicates that bridging hydroxyl groups in zeolites X and erionite are preferentially formed at oxygen bridges to Si(nAl) sites with a maximum number n of framework aluminium atoms in the second co-ordination sphere of silicon [37].

Two-dimensional ^{29}Si CP/MAS spectra of zeolites were measured by Vega [119]. In heteronuclear chemical shift correlation spectra of hydrated zeolites CaNaA and HRHO Vega identified hydroxyl protons of silanol groups which were rigidly bound to silicon atoms of hydrated and dehydrated zeolite frameworks. A homonuclear two-dimensional ^{1}H experiment was used to detect the proton spin exchange.

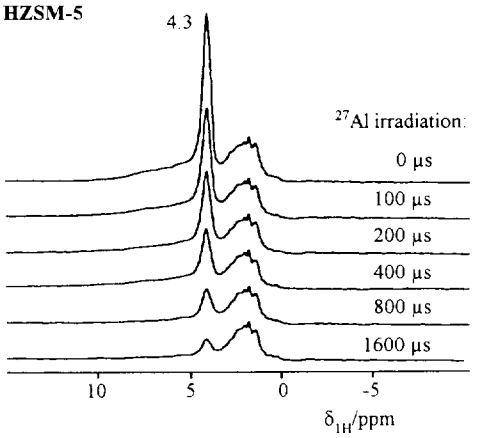


Fig. 18. ^{1}H MAS spectra of dehydrated (673 K) zeolite HZSM-5 (Si/Al = 23) recorded at 500.13 MHz, a MAS frequency ν_{rot} of 10 kHz and using a dipolar-dephasing spin-echo sequence with ^{27}Al irradiation of pulse lengths in the range 0–1600 μs [77].

Beck and co-workers [76,150] applied a dipolar-dephasing spin-echo MAS sequence to distinguish lines from hydroxyl protons in zeolites HZSM-5 and HBeta which interact with heteronuclei. In these ^{1}H MAS studies, ^{27}Al dephasing pulses were applied during the pulse and echo delays of a rotation-synchronized Hahn echo. Fig. 18 shows the ^{1}H dipolar dephasing spin-echo MAS spectra of dehydrated zeolite HZSM-5 (Si/Al = 23) recorded by Freude [77] using the same technique. An increase in the ^{27}Al irradiation time from 0 to 1600 μs produces a strong decrease in the intensity of the line at 4.3 ppm, which indicates the dipolar interaction of these hydroxyl groups with the ^{27}Al nuclei. An additional advantage of the spin-echo sequence is the enhanced resolution of the ^{1}H MAS lines of the silanol groups.

Most of the ^{1}H MAS spectra of dehydrated aluminosilicates and silicoaluminophosphates show lines from SiOH groups at 1.4–2.2 ppm. The question arises whether these defect OH

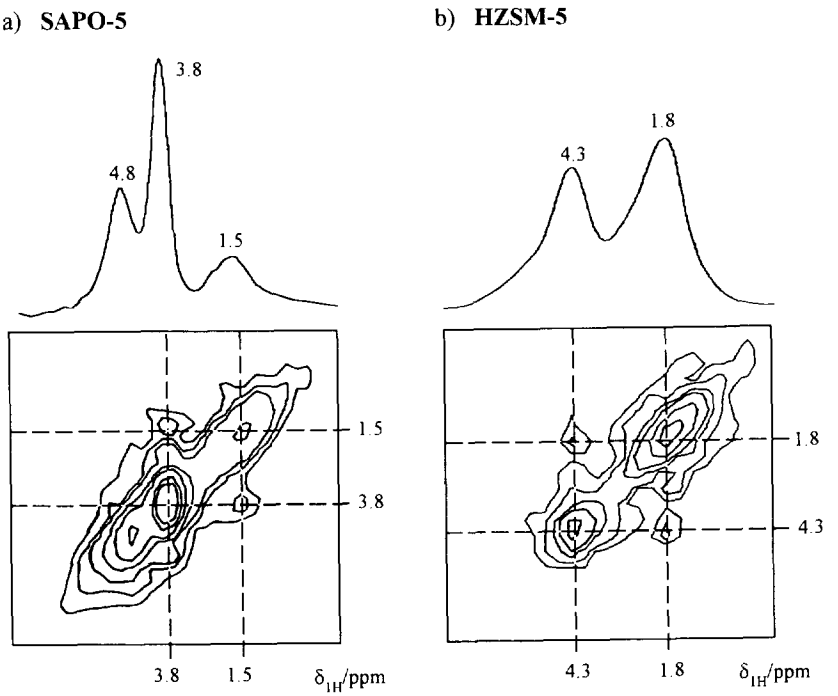
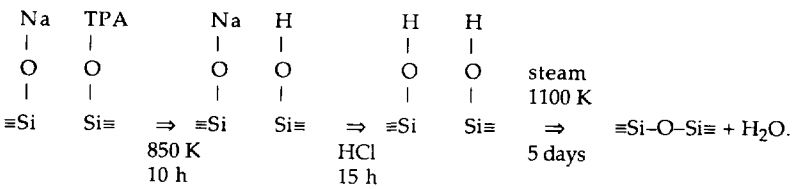


Fig. 19. Contour plots of the two-dimensional ^{1}H MAS NOESY spectra of hydroxyl protons in (a) SAPO-5 [122] and (b) HZSM-5 [151] dehydrated at 673 K, recorded at 300.13 MHz with MAS frequency ν_{rot} of 3 kHz and a mixing time of 50 ms. The dotted lines are drawn at the chemical shifts of the SiOH groups at 1.5 ppm (a) and 1.8 ppm (b) and of the bridging OH groups at 3.8 ppm (a) and 4.3 ppm (b), which are responsible for the appearance of cross-peaks.

groups are located at the outer surface of the zeolitic particles or in intact channels or cavities, i.e. in the neighbourhood of bridging OH groups. The location of these SiOH groups at framework defects was studied using two-dimensional homonuclear spin diffusion (NOESY [121,122]). Fig. 19(a) shows the NOESY spectrum of hydroxyl protons in dehydrated silicoaluminophosphate SAPO-5 recorded at the ^{1}H frequency of 300.13 MHz, MAS frequency of 3 kHz and with a mixing time of 50 ms. The ^{1}H MAS spectra of dehydrated SAPO-5 consist of lines of SiOH groups at 1.5 ppm and of bridging OH groups in 12-ring channels and six-membered oxygen rings at 3.8 and 4.8 ppm [37,80,123], respectively. The two-dimensional NOESY cross-peaks caused by the lines at 1.5 and 3.8 ppm (Fig. 19(a)) indicate the closeness of the SiOH groups and bridging



Scheme 1.

OH groups in the 12-ring channels. The existence of a large number of silanol groups at the outer surface or at silicon-rich islands in SAPO-5 can, therefore, be excluded.

Synthesis of zeolite ZSM-5 using tetrapropylammonium iodide or bromide (TPA^+) as a structure-directing agent yields zeolite particles with defect Si–O–Si bonds [120,124–126]. Up to 8% of the silicon atoms in these zeolites are involved in defect SiOH groups. Analysis of the ^1H MAS data suggests the reaction scheme shown in Scheme 1 of defect sites in the "as-synthesized" zeolite TPA^+/ZSM-5, after thermal decomposition of the template, and after acid leaching and steaming [120,125]. This scheme is supported by the ^{29}Si CP/MAS NMR and Fourier transform infra-red (FTIR) spectroscopy results reported by Woolery et al. [127] and Groenen et al. [128]. Fig. 19(b) shows a homonuclear two-dimensional NOESY spectrum of hydroxyl protons in dehydrated HZSM-5 (Si/Al = 40), showing cross-peaks for the ^1H MAS lines from SiOH groups at 1.8 ppm and from bridging OH groups at 4.3 ppm, which indicates that the two types of hydroxyl proton are close neighbours. As the hydroxyl protons of bridging OH groups point into the 10-ring channels of HZSM-5, silanol groups at the defect Si–O–Si bonds are also located inside the channels. This result accounts for the appearance of silanol groups upon thermal decomposition of TPA^+ ions (see Scheme 1), these groups being located at the channel intersections in the "as-synthesized" TPA^+/ZSM-5.

6. Local structure of OH groups in zeolites

6.1. Silanol groups in zeolite HZSM-5

The second moment of the ^1H line [129] of silanol groups in HZSM-5 synthesized with TPA^+ is determined by the H–H distance (r_{HH}) of two neighbouring hydroxyl protons within SiOH pairs. For hydrogen-exchanged HZSM-5 with Si/Al = 176, the measured second moment M_2^{exp} is 4.0×10^{-9} T^2 [126]. In view of the negligibly small dipolar H–Si interaction ($M_2^{HSi} = 0.02 \times 10^{-9}$ T^2) and the low framework aluminium content ($M_2^{HAl} \approx 0$), the second moment M_2^{exp} originates exclusively from dipolar H–H interactions between the hydroxyl protons within the SiOH pairs ($M_2^{exp} = M_2^{HH}$). As [126,130]

$$M_2^{HH}/10^{-14}\ T^2 = 358.1 r_{HH}^{-6}/nm^{-6} \quad (11)$$

the pairwise H–H distance is $r_{HH} = 0.32$ nm. As SiOH pairs can be considered as spin pairs, the decay of the amplitudes of Hahn echoes yields the density ρ of spin pairs [126,131]:

$$T_2^{Hahn}/s = 0.347(\rho/nm^{-3})^{-1} \quad (12)$$

Using Eq. (12), the measured value of $T_2^{Hahn} = 0.375$ s corresponds to the density of SiOH pairs of $\rho = 0.92$ nm^{-3} or a mean number of about 0.7 spin pairs per channel intersection [126]. This number of SiOH pairs decreases strongly after steaming at 1100 K [125], which indicates a healing of up to 50% of defective Si–O–Si bonds (see Scheme 1).

6.2. Local structure of bridging OH groups

Using neutron diffraction, Czjzek et al. [30] and Bull et al. [29] examined the geometry of bridging OH groups in faujasite-type zeolites HNaY and SAPO-37. From the mean bond lengths and angles of the local structure of the bridging OH groups, as determined by neutron diffraction, the mean H–T distance (T = Si or Al) in zeolites HY and SAPO-37 is $r_{HT} = 0.222$ nm. The occupation of the proton sites at the O1, O2 and O3 bridging oxygen atoms was determined for both zeolites [29,30]. The T–O3–T bond angles were found to be 4–7° larger than those of the T–O1–T bridges. Quantum chemical calculations yielded H–Al distances within bridging OH groups in zeolite HY of 0.239 and 0.233 nm for SiO1HAl and SiO3HAl groups, respectively [7,8]. Curtiss et al. [10] have reported a local structure for SiOHAl groups, with a H–Al distance of 0.255 nm (derived using ab initio methods). In agreement with these experimental methods the energy minimization of the lattice of zeolite HY [8] yielded a preferred occupation of proton sites at O1 and O3 framework oxygen atoms.

Stevenson [132] measured the second moment M_2^{HAl} of the broad-line ^1H line of the bridging

OH groups in dehydrated zeolite HY and calculated the H–Al distance r_{HAl} to be 0.238 nm. This value was verified by Freude et al. [133,134] using the same method. A larger H–Al distance of $r_{HAl} = 0.248$ nm was found for bridging OH groups in dehydrated zeolite HZSM-5 (Si/Al = 15). Kenaston et al. [135] applied spin-echo double resonance (SEDOR) to determine the H–Al distance of the bridging OH groups in dehydrated HZSM-5 (Si/Al = 30). Spin-echos of ^{27}Al nuclei with and without irradiation of ^{1}H pulses during the ^{27}Al pulse delays were measured. An H–Al distance r_{HAl} of 0.2430 ± 003 nm was calculated by fitting the decays of the SEDOR echo areas as a function of the ^{1}H pulse delays. The H–Al distance r_{HAl} of 0.2460 ± 003 nm was derived [135] from the second moment M_2^{HAl} of the wide-line ^{1}H line of the same sample.

The ^{1}H MAS side-band patterns of bridging OH groups were analysed to determine the second moment of the dipolar H–Al interaction and the anisotropy of chemical shift $\Delta\sigma_{OH}$ of hydroxyl protons in bridging OH groups [37,136,137]. An important advantage of this method is the selec-

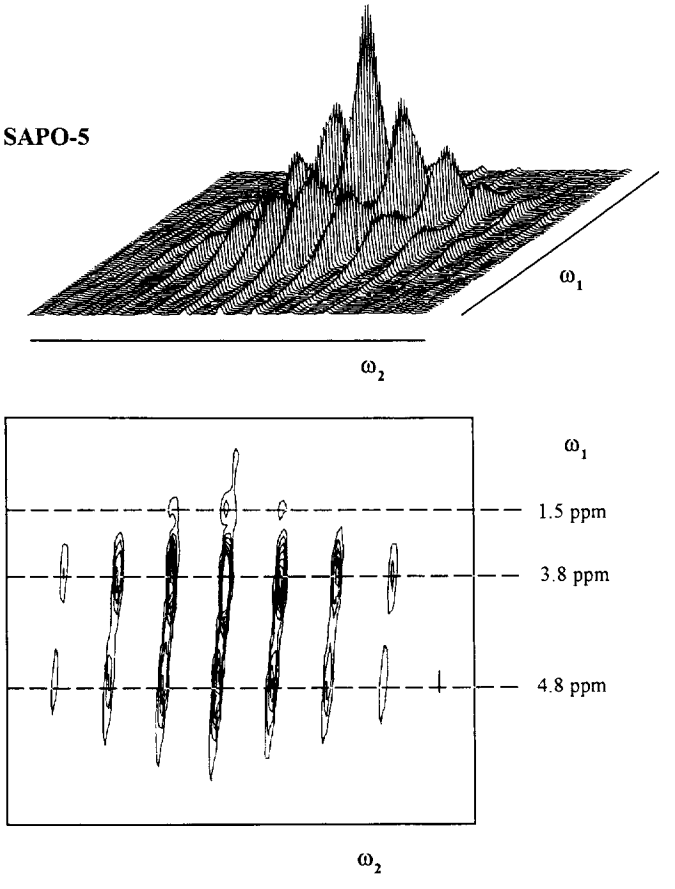


Fig. 20. Stacked plot (top) and contour plot (bottom) of the two-dimensional ^{1}H MAS spectrum of silicoalmuninophosphate SAPO-5 dehydrated at 673 K (from Refs. [37] and [136]). The spectra were recorded at 300.13 MHz, a MAS frequency ν_{rot} of 2 kHz and using a rotation-synchronized pulse sequence with multiples of $1/\nu_{rot}$ as a maximum of 64 increments in the period t_1 (see text) to eliminate MAS modulation in the ω_1 dimension [151].

tive analysis of MAS sideband patterns of the ^{1}H MAS lines caused by hydroxyl protons appearing at different isotropic chemical shifts. The NMR parameters can therefore be derived selectively for bridging OH groups located in supercages or channels and in small cavities or six-membered oxygen rings, as found in zeolites HY, erionite, SAPO-5, SAPO-17 (structure type ERI) and SAPO-37 (structure type FAU) [37,137]. The MAS side-band patterns of lines appearing at different isotropic chemical shifts were separated by a rotation-synchronized two-dimensional pulse experiment. The time period t_1 after the $\pi/2$ pulse excitation is incrementally increased using the MAS spinning period τ_{rot} as the increment ($t_1 = n\tau_{rot}$). As proposed by Aue et al. [138], a π pulse was given at the end of period t_1. Aquisition (t_2) was started immediately after the π pulse. Two-fold Fourier transformation of $G(t_1, t_2)$ recorded using this pulse experiment yields a two-dimensional spectrum $F(\omega_1, \omega_2)$ which has no MAS modulation in the ω_1 dimension (Fig. 20, top). Slices on the ω_1 axis at the isotropic chemical shift values of hydroxyl protons yield separated MAS side-band patterns of the lines of bridging OH groups (Fig. 20, bottom).

To simulate the ^{1}H MAS side-band patterns of bridging OH groups, the following expression of the free induction decay was used [37,136,137]:

$$G(t) = G^{ext}(t)\left\langle\left\langle \exp\left(-i\int_0^t \omega(t)\,dt\right)\right\rangle\right\rangle_{powder}\Big\rangle_{m_S} \tag{13}$$

With the chemical shift tensor $\boldsymbol{T}$(CSA) and the traceless tensor $\boldsymbol{T}(M_2^{HAl})$ of the dipolar H–Al interaction, the frequency function in Eq. (13) becomes

$$\omega(t) = \left\{\boldsymbol{b}(t)\left[\boldsymbol{T}(\mathrm{CSA}) + m_S\boldsymbol{T}\left(M_2^{HAl}\right)\right]\boldsymbol{b}(t)\right\} \tag{14}$$

where $\boldsymbol{b}$(t) denotes the unit vector along the direction of the magnetic field in the axes system of the bridging OH group, which becomes a periodic function of time under MAS conditions. The quantum number of the ^{27}Al nucleus (spin S) is considered via the value of m_S. The factor:

$$G^{ext}(t) = \exp\left\{-\frac{M_2^{ext}}{\omega_{rot}^2}\frac{2}{3}\left[1-\cos(\omega_{rot}t)\right] + \frac{1}{12}\left[1-\cos(2\omega_{rot}t)\right]\right\} \tag{15}$$

accounts for the homonuclear and heteronuclear dipole–dipole interactions between the hydroxyl protons of bridging OH groups and the external nuclei outside the local structure (M_2^{ext}). Finally, the experimental ^{1}H MAS side-band patterns were fitted by patterns calculated from Eq. (13). The values of $r_{HAl}(M_2^{HAl})$ and $\Delta\sigma_{OH}$ were determined using the least-squares method for both data sets.

Table 1 summarizes the experimentally derived H–Al distances of bridging OH groups in various aluminosilicates and silicoaluminophosphates taken from Ref. [37]. The values of M_2^{ext} are $(0.5 \pm 0.3) \times 10^8$ s^{-2} for aluminosilicates with Si/Al ratios of 1.0–2.9 and $(1.0 \pm 0.3) \times 10^8$ s^{-2} for aluminosilicates with Si/Al ratios higher than 7.1 and for silicoaluminophosphates. The values of the chemical shift anisotropies $\Delta\sigma_{OH}$ cover a range between 13.5 and 17.5 ppm. Fig. 21 shows the relation between the H–Al distances in the local structure of the bridging OH groups and the types of oxygen ring in which these hydroxyl

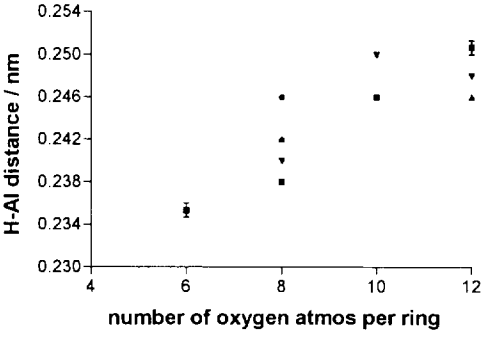


Fig. 21. Experimentally derived H–Al distances r_{HAl} of bridging OH groups as a function of the number of oxygen atoms per oxygen ring in which the hydroxyl protons are located (see columns 3 and 8, Table 1).

protons are located (columns 3 and 8, Table 1). It is interesting to note that the difference of the H–Al distances of SiO1HAl ($r_{HAl} = 0.250 \pm 0.002$ nm) and SiO3HAl ($r_{HAl} = 0.235 \pm 0.002$ nm) groups in zeolites HY and SAPO-37 agrees qualitatively with the values derived using a quantum-chemical calculation ($r_{HAl} = 0.239$ nm and $r_{HAl} = 0.233$ nm) [7,8]. The same relation follows from the T–O1–T and T–O3–T bond angles of the bridging OH groups in zeolites HY and SAPO-37 as determined by neutron diffraction, which cover a range 135.7–137.9° for SiO1HAl and 139.8–144.5° [29,30] for the SiO3HAl groups.

Using MAS NMR side-band analysis, Koch et al. [86] studied the influence of CO adsorption on the H–Al distance of bridging OH groups in zeolite HZSM-5. For unloaded and loaded (about 1 equivalent of CO) zeolite HZSM-5 the same H–Al distance r_{HAl} of 0.253 ± 0.002 nm was determined. However, after adsorption of CO, the chemical anisotropy $\Delta\sigma_{OH}$ increases significantly from 14 ± 2 to 22 ± 2 ppm, due to the formation of a linear adsorbate complex. In addition, the equilibrium distance r_{HC} between the hydroxyl proton and the carbon atom of the probe molecule was studied at 123 K. The second moment M_2 of the ^{1}H line of bridging OH groups interacting with carbon monoxide is given by:

$$M_2^{13C} = M_2^{12C} + M_2^{H-C} \tag{16}$$

where M_2^{12C} and M_2^{13C} are the second moments of the ^{1}H line of the bridging hydroxyl groups in HZSM-5 loaded with ^{12}CO and ^{13}CO, respectively, and M_2^{CH} is given by [86]

$$M_2^{H-C}/s^{-2} = 7.19 \times 10^3 \left[p\left(r_{H-C}/nm^{-6}\right)^{-6} + (1-p)(r_{H-O} + r_{CO})/nm^{-6} \right]^{-6} \tag{17}$$

where p denotes the fraction of CO molecules bonded to bridging OH groups via the carbon atoms forming ZOH–CO complexes, as opposed to the fraction $(1-p)$ which form ZOH–OC complexes; r_{CO} is the C–O distance in carbon monoxide (0.113 nm). The values of M_2^{12C} and M_2^{13C} were measured by analysing the ^{1}H MAS side-band patterns of zeolite HZSM-5 loaded with ^{12}CO and ^{13}CO. The value $M_2^{HC} = 0.64 \times 10^8$ s^{-2} was determined using Eq. (16). Assuming $p \approx 0.5$ and $r_{H-C} \approx r_{H-O}$, the H–C distance between the carbon atoms of adsorbed CO molecules and the hydroxyl protons of bridging OH groups is $r_{H-C} = 0.20 \pm 0.02$ nm (Eq. (17)), which is in good agreement with the H–C distances obtained from quantum chemical calculations by Beran [139] and Gerlings et al. [140].

The magnitude of the electric field gradients at the sites of the hydroxyl protons is sensitive to the charge distribution in the local structure of the OH groups in zeolites and has been studied using ^{2}H NMR on deuterated samples. From the static ^{2}H spectrum of zeolite Y exchanged with ND_4NO_3 and calcined at 723 K, Gluszak et al. [141] determined a quadrupole coupling constant of ^{2}H in SiODAl groups as QCC = 234 ± 2 kHz. Ernst et al. [19] and Freude et al. [142] recorded the ^{2}H MAS spectra of a dehydrated zeolite deuterated by adsorption of D_2O and subsequently calcined. Dividing the MAS side-band spectrum of the one-dimensional ^{2}H MAS spectra into single side-band files, they generated two-dimensional plots which show the deuterium NMR shift of the OD groups in the ω_1 dimension and the quadrupole frequency of the deuterons in the ω_2 dimension. For deuterons of bridging OD groups in zeolites 50HNaX (Si/Al = 1.4), 92HNaY (Si/Al = 3.1) and HZSM-5 (Si/Al = 22.0) they obtained quadrupole coupling constants QCC of 236 ± 10, 224 ± 10 and 208 ± 10 kHz, respectively, and suggest that small quadrupole coupling constants found for SiODAl groups in zeolites with low framework aluminium content correspond to high acid strengths of the Brønsted centres, and vice versa.

Acknowledgements

I am grateful to Professors H. Pfeifer (University of Leipzig) and D. Freude (University of Leipzig) and to Dr. G. Engelhardt (University of Stuttgart) for discussions, and to the Deutsche Forschungsgemeinschaft and the Max Buchner-Forschungsstiftung for support.

References

[1] J. Weitkamp, H.G. Karge, H. Pfeifer and W. Hölderich (Eds.), Zeolites and Related Microporous Materials: State of Art 1994, Studies in Surface Science and Catalysis, Vol. 84a–84c, Elsevier, Amsterdam, 1994.

[2] P.B. Venuto, Microporous Mater., 2 (1994) 297.

[3] J.A. Rabo and G.J. Gajda, Catal. Rev.-Sci. Eng., 31 (1989–1990) 385.

[4] J.A. Rabo, Zeolite Chemistry and Catalysis, ACS Monograph 171, American Chemical Society, Washington, DC, 1976.

[5] P.B. Venuto and E.T. Habib, Fluid Catalytic Cracking with Zeolite Catalysts, Marcel Dekker, New York, 1978.

[6] N.Y. Chen, W.E. Garwood and F.G. Dwyer, Selective Catalysis in Industrial Applications, Marcel Dekker, New York, 1989.

[7] J. Sauer, in J. Weitkamp, H.G. Karge, H. Pfeifer and W. Hölderich (Eds.), Zeolites and Related Microporous Materials: State of Art 1994, Studies in Surface Science and Catalysis, Vol. 84, Elsevier, Amsterdam, 1994, p. 2039.

[8] K.-P. Schröder, J. Sauer, M. Leslie, C.R.A. Catlow and J.M. Thomas, Chem. Phys. Lett., 188 (1992) 320.

[9] R.A. van Santen, A.J.M. de Man, W.P.J.H. Jacobs, E.H. Teunissen and G.J. Kramer, Catal. Lett., 9 (1991) 273.

[10] L.A. Curtiss, H. Brand, J.B. Nicholas and L.E. Iton, Chem. Phys. Lett., 184 (1991) 215.

[11] J.B. Nicholas and A.C. Hess, J. Am. Chem. Soc., 116 (1994) 5428.

[12] U. Fleischer, W. Kutzelnigg, A. Bleiber and J. Sauer, J. Am. Chem. Soc., 115 (1993) 7833.

[13] F. Haase and J. Sauer, J. Phys. Chem., 98 (1994) 3083.

[14] E.H. Teunissen, R.A. van Santen and A.P.J. Jansen, J. Phys. Chem., 97 (1993) 203.

[15] F. Haase and J. Sauer, J. Am. Chem. Soc., 117 (1995) 3780.

[16] J.D. Gale, C.R.A. Catlow and J.R. Catlow, Chem. Phys. Lett., 216 (1993) 155.

[17] D. Freude, M. Hunger and H. Pfeifer, Chem. Phys. Lett., 91 (1982) 307.

[18] H. Pfeifer, D. Freude and M. Hunger, Zeolites, 5 (1985) 274.

[19] H. Ernst, D. Freude and I. Wolf, Chem. Phys. Lett., 212 (1993) 588.

[20] H. Pfeifer, Colloids Surf., 36 (1989) 169.

[21] H. Pfeifer, NMR Basic Principles and Progress, Vol. 31, Springer-Verlag, Berlin, 1994, p. 31.

[22] H. Pfeifer and H. Ernst, Ann. Rep. NMR Spectrosc., 28, (1994) 91.

[23] J. Yesinowski, H. Eckert and G.R. Rossman, J. Am. Chem. Soc., 110 (1987) 1369.

[24] S.F. Dec, C.E. Bronnimann, R.A. Wind and G.E. Maciel, J. Magn. Reson., 82 (1989) 454.

[25] E. Brunner, J. Chem. Soc., Faraday Trans., 89 (1993) 165.

[26] M. Hunger, Habilitation Thesis, Institute of Physics, University of Leipzig, 1991.

[27] J.W. Ward, in J.A. Rabo (Ed.), Zeolite Chemistry and Catalysis, ACS Monograph 171, American Chemical Society, Washington, DC, 1976, p. 118.

[28] P.A. Jacobs and W.J. Mortier, Zeolites, 2 (1982) 226.

[29] L.M. Bull, A.K. Cheetham, P.D. Hopkins and B.M. Powell, J. Chem. Soc., Chem. Commun., (1993) 1196.

[30] M. Czjzek, H. Jobic and A.N. Fitch, T. Vogt, J. Phys. Chem., 96 (1992) 1535.

[31] D. Freude, M. Hunger, H. Pfeifer, G. Scheler, J. Hoffmann and W. Schmitz, Chem. Phys. Lett., 105 (1984) 427.

[32] M. Hunger, D. Freude, H. Pfeifer, D. Prager and W. Reschetilowski, Chem. Phys. Lett., 163 (1989) 221.

[33] V.M. Mastikhin, I.L. Mudrakovsky and A.V. Nosov, Prog. NMR Spectrosc., 23 (1991) 259.

[34] E.T. Olejniczak, S. Vega and R.G. Griffin, J. Chem. Phys., 81 (1984) 4804.

[35] D. Freude, M. Hunger and H. Pfeifer, Z. Phys. Chem. (NF), 152 (1987) 429.

[36] D. Freude, M. Hunger, H. Pfeifer and W. Schwieger, Chem. Phys. Lett., 128 (1986) 62.

[37] M. Hunger, M.W. Anderson, A. Ojo and H. Pfeifer, Microporous Mater., 1 (1993) 17.

[38] R.T. Sanderson, Chemical Bonds and Bond Energy, Academic Press, New York, 1976.

[39] M.A. Makarova, A.F. Ojo, K. Karim, M. Hunger and J. Dwyer, J. Phys. Chem., 98 (1994) 3619.

[40] M.J.P. Brugmans, A.W. Kleyn, A. Lagendijk, W.P.J.H. Jacobs and R.A. van Santen, Chem. Phys. Lett., 217 (1994) 117.

[41] J.P. Yesinowski and H. Eckert, J. Am. Chem. Soc., 109 (1987) 6274.

[42] M.L. Costenoble, W.J. Mortier and J.B. Uytterhoeven, J. Chem. Soc., Faraday Trans. I, 174 (1978) 466, 477.

[43] M. Hunger and T. Horvath, Ber. Bunsenges. Phys. Chem. 99(11) (1995) 1316.

[44] U. Lohse, E. Löffler, M. Hunger, J. Stöckner and V. Patzelova, Zeolites, 7 (1987) 11.

[45] G. Engelhardt, H.-G. Jerschkewitz, U. Lohse, P. Sarv, A. Samoson and E. Lippmaa, Zeolites, 7 (1987) 291.

[46] E. Brunner, H. Ernst, D. Freude, M. Hunger, C.B. Krause, D. Prager, W. Reschetilowski, W. Schwieger and K.-H. Bergk, Zeolites, 9 (1989) 282.

[47] E. Brunner, H.G. Karge and H. Pfeifer, Z. Phys. Chem., 176 (1992) 173.

[48] P.H. Kasai and P.M. Jones, J. Mol. Catal., 27 (1984) 81.

[49] K.F.M.G.J. Scholle, W.S. Veeman, J.G. Post and J.H.C. van Hooff, Zeolites, 3 (1983) 214.

[50] K.F.M.G.J. Scholle, A.P.M. Kentgens, W.S. Veeman, P. Frenken and G.P.M. van der Velden, J. Phys. Chem., 88 (1984) 5.

[51] C.I. Ratcliffe, J.A. Ripmeester and J.S. Tse, Chem. Phys. Lett., 120 (1985) 427.

[52] M. Hunger, D. Freude and H. Pfeifer, J. Chem. Soc., Faraday Trans., 87 (1991) 657.

[53] P. Batamack, C. Doremieux-Morin, J. Fraissard and D. Freude, J. Phys. Chem., 95 (1991) 3790.
[54] R. Challoner, R.K. Harris, S.A.I. Barri and M.J. Taylor, Zeolites, 11 (1991) 827.
[55] M. Hunger, D. Freude, T. Fröhlich, H. Pfeifer and W. Schwieger, Zeolites, 7 (1987) 108.
[56] A.E. Hirschler, J. Catal., 2 (1963) 428.
[57] C.J. Plank, Proceedings of the Third International Congress on Catalysis, Amsterdam, Vol. 1, p. 727.
[58] R. Schlunk, Diploma Thesis, Institute of Chemical Technology I, University of Stuttgart, 1994.
[59] B. Staudte, M. Hunger and M. Nimz, Zeolites, 11 (1991) 837.
[60] D.H. Olson and E. Dempsey, J. Catal., 13 (1969) 221.
[61] W.J. Mortier, J. Pluth and J.V. Smith, J. Catal., 45 (1976) 367.
[62] Z. Jirak, S. Vratislav and V. Bosacek, J. Phys. Chem. Solids, 41 (1980) 1089.
[63] M. Czjzek, H. Jobic, A.N. Fitch and T. Voigt, J. Phys. Chem., 96 (1992) 1535.
[64] E. Brunner, Microporous Mater., 1 (1993) 431.
[65] J. Klinowski, H. Hamdan, A. Corma, V. Fornes, M. Hunger and D. Freude, Catal. Lett., 3 (1989) 263.
[66] W. Reschetilowski, W.-D. Einicke, M. Jusek, R. Schöllner, D. Freude, M. Hunger and J. Klinowski, Appl. Catal., 56 (1989) L15.
[67] D. Freude, T. Fröhlich, M. Hunger, H. Pfeifer and G. Scheler, Chem. Phys. Lett., 98 (1983) 263.
[68] J.B. Uytterhoeven, L.G. Christner and W.K. Hall. J. Phys. Chem., 69 (1965) 2177.
[69] A.J. Vega and Z. Luz, J. Phys. Chem., 91 (1987) 365.
[70] R.D. Shannon, R.H. Staley, A.J. Vega, R.X. Fischer, W.H. Baur and A. Auroux, J. Phys. Chem., 93 (1989) 2019.
[71] F. Roessner, K.-H. Steinberg, D. Freude, M. Hunger and H. Pfeifer, in H.G. Karge and J. Weitkamp (Eds.), Zeolites as Catalysts, Sorbents and Detergent Builders, Elsevier, Amsterdam, 1989, p. 421.
[72] P.G. Clarke, K. Gosling, R.K. Harris and E.G. Smith, Zeolites, 13 (1993) 388.
[73] E. Brunner, H. Ernst, D. Freude, T. Fröhlich, M. Hunger and H. Pfeifer, in P.A. Jacobs and R.A. van Santen (Eds.), Studies in Surface Science and Catalysis, Vol. 49, Elsevier, Amsterdam, 1989, p. 623.
[74] M. Hunger, D. Freude and H. Pfeifer, Catal. Today, 3 (1988) 507.
[75] E. Brunner, K. Beck, L. Heeribout and H.G. Karge, Microporous Mater., 3 (1995) 395.
[76] L.W. Beck, J.L. White and J.F. Haw, J. Am. Chem. Soc., 116 (1994) 9657.
[77] D. Freude, Chem. Phys. Lett., 235 (1995) 69.
[78] T. Ikenoue and N. Yoshida, J. Phys. Chem., 92 (1988) 4883.
[79] M. Hunger, T. Horvath, G. Engelhardt and H.G. Karge, in H.K. Beyer, H.G. Karge, I. Kiricsi and J.B. Nagy (Eds.), Catalysis by Microporous Materials, Studies in Surface Science and Catalysis, Vol. 94, Elsevier, Amsterdam, 1995, p. 756.
[80] B. Zibrowius, E. Löffler and M. Hunger, Zeolites, 12 (1992) 167.
[81] H. Ernst, D. Freude, M. Hunger, H. Pfeifer and B. Seiffert, Z. Phys. Chem. (Leipzig), 268 (1987) 304.
[82] W.P.J.H. Jacobs, J.W. de Haan, L.J.M. van de Ven and R.A. van Santen, J. Phys. Chem., 97 (1993) 10394.
[83] M. Hunger, S. Ernst and J. Weitkamp, Zeolites, 15 (1995) 188.
[84] J.L. White, L.W. Beck and J.F. Haw, J. Am. Chem. Soc., 114 (1992) 6182.
[85] J.F. Haw, M.B. Hall, A.E. Alvarado-Swaisgood, E.J. Munson, Z. Lin, L.W. Beck and T. Howard, J. Am. Chem. Soc., 116 (1994) 7308.
[86] M. Koch, E. Brunner, D. Fenzke, H. Pfeifer and B. Staudte, Studies Surf. Sci. Catal., 84 (1994) 709.
[87] E. Brunner, K. Beck, M. Koch, H. Pfeifer, B. Staudte and D. Zscherpel, Studies Surf. Sci. Catal., 84 (1994) 357.
[88] J.A. Ripmeester, J. Am. Chem. Soc., 105 (1983) 2925.
[89] D. Schulze, H. Ernst, D. Fenzke, W. Meiler and H. Pfeifer, J. Phys. Chem., 94 (1990) 3499.
[90] W.P. Rothwell, W.X. Shen and J.H. Lunsford, J. Am. Chem. Soc., 106 (1984) 2452.
[91] J.H. Lunsford, W.P. Rothwell and W. Shen, J. Am. Chem. Soc., 107 (1985) 1540.
[92] J.H. Lunsford, P.N. Tutunjian, P.-J. Chu, E.B. Yeh and D.J. Zalewski, J. Phys. Chem., 93 (1989) 2590.
[93] R. Carvajal, P.-J. Chu and J.H. Lunsford, J. Catal., 125 (1990) 123.
[94] J.H. Lunsford, H. Sang, S.M. Campbell, C.-H. Liang and RG. Anthony, Catal. Lett., 27 (1994) 305.
[95] H. Sang, H.Y. Chu and J.H. Lunsford, Catal. Lett., 26 (1994) 235.
[96] A.I. Biaglow, R.J. Gorte, G.T. Kokotailo and D. White, J. Catal., 148 (1994) 779.
[97] J. Sauer, C. Kölmel, F. Haase and R. Ahlrichs, Proceedings of the 9th International Zeolite Conference, Montreal, 1992, Butterworth-Heinemann, Boston, 1993, p. 679.
[98] J. Sauer, H. Horn, M. Häser and R. Ahlrichs, Chem. Phys. Lett., 173 (1990) 26.
[99] J. Sauer, J. Acta. Chim. Phys., Szeged, 31 (1985) 19.
[100] J. Sauer and P. Hobza, Theor. Chim. Acta (Berlin), 65 (1984) 279, 291.
[101] C. Doremieux-Morin, J. Magn. Reson., 21 (1976) 419.
[102] C. Doremieux-Morin, J. Magn. Reson., 33 (1979) 505.
[103] P. Batamack, C. Doremieux-Morin, R. Vincent and J. Fraissard, Chem. Phys. Lett., 180 (1991) 545.
[104] P. Batamack, C. Doremieux-Morin, R. Vincent and J. Fraissard, J. Phys. Chem., 97 (1993) 9779.
[105] P. Batamack, C. Doremieux-Morin, R. Vincent and J. Fraissard, Microporous Mater., 2 (1994) 515.
[106] V.M. Mastikhin and O.B. Lapina, React. Kinet. Lett., 11 (1979) 353.

[107] R.K. Harris and B.E. Mann (Eds.), NMR and the Periodic Table, Academic Press, New York, 1979, p. 89.
[108] J.W. Emsley, J. Feeney and L.M. Sutcliffe, High Resolution NMR Spectroscopy, Pergamon Press, Oxford, 1966, p. 263.
[109] S.L. Meisel, J.P. McCullogh, C.H. Lechthaler and P.B. Weisz, Chemtech, 6 (1976) 86.
[110] W.W. Kaeding and S. Butter, U.S. Patent 3 911 041 (1975).
[111] Z. Luz and A.J. Vega, J. Phys. Chem., 91 (1987) 374.
[112] J. Klinowski and M.W. Anderson, Magn. Reson. Chem., 28 (1990) S68.
[113] G. Mirth, J.A. Lercher, M.W. Anderson and J. Klinowski, J. Chem. Soc., Faraday Trans., 86 (1990) 3039.
[114] M.W. Anderson, P.J. Barrie and J. Klinowski, J. Phys. Chem., 95 (1991) 235.
[115] H. Ernst, D. Freude and T. Mildner, Chem. Phys. Lett., 229 (1994) 291.
[116] D.W. Breck, Zeolite Molecular Sieves, Robert E. Krieger, Malabar, FL, 1984, p. 636.
[117] W.M. Meier and D.H. Olson, Atlas of Zeolite Structure Types, Butterworths, London, 1987.
[118] G. Engelhardt, U. Lohse, A. Samoson, M. Mägi, M. Tarmak and E. Lippmaa, Zeolites, 2 (1982) 59.
[119] A.J. Vega, J. Am. Chem. Soc., 110 (1988) 1049.
[120] G. Engelhardt, B. Fahlke, M. Mägi and E. Lippmaa, Z. Phys. Chem. (Leipzig), 266 (1985) 239.
[121] R.R. Ernst, Chimia, 41 (1987) 323.
[122] E. Brunner, D. Freude, M. Hunger, H. Pfeifer and B. Staudte, Studies Surf. Sci. Catal., 69 (1991) 453.
[123] D. Freude, H. Ernst, M. Hunger, H. Pfeifer and E. Jahn, Chem. Phys. Lett., 143 (1988) 477.
[124] W. Schwieger, K.-H. Bergk, D. Freude, M. Hunger and H. Pfeifer, ACS Symp. Ser., 398 (1989) 274.
[125] M. Hunger, J. Kärger, H. Pfeifer, J. Caro, B. Zibrowius, M. Bülow and R. Mostowicz, J. Chem. Soc., Faraday Trans. 1, 83 (1987) 3459.
[126] M. Hunger, D. Freude, H. Pfeifer and W. Schwieger, Chem. Phys. Lett., 167 (1990) 21.
[127] G.L. Woolery, L.B. Alemany, R.M. Dessau and A.W. Chester, Zeolites, 6 (1986) 14.
[128] E.J.J. Groenen, A.G.T.G. Kortbeek, M. Mckay and O. Sudmeijer, Zeolites, 6 (1986) 403.
[129] A. Abragam, The Principles of Nuclear Magnetism, Clarendon Press, Oxford, 1962.
[130] D. Freude and H. Schmiedel, Phys. Stat. Sol. (b), 54 (1972) 631.
[131] D. Freude, Adv. Colloid Interface Sci., 23 (1985) 21.
[132] R.L. Stevenson, J. Catal., 21 (1971) 113.
[133] D. Freude, J. Klinowski and H. Hamdan, Chem. Phys. Lett., 149 (1988) 355.
[134] D. Freude and J. Klinowski, J. Chem. Commun., (1988) 1411.
[135] N.P. Kenaston, A.T. Bell and J.A. Reimer, J. Phys. Chem., 98 (1994) 894.
[136] D. Fenzke, M. Hunger and H. Pfeifer, J. Magn. Reson., 95 (1991) 477.
[137] M. Hunger, D. Freude, D. Fenzke and H. Pfeifer, Chem. Phys. Lett., 191 (1992) 391.
[138] W.P. Aue, D.J. Ruben and R.G. Griffin, J. Magn. Reson., 43 (1981) 472.
[139] S. Beran, J. Phys. Chem., 87 (1983) 55.
[140] P. Geerlings, N. Tariel, A. Botrel, R. Lissilour and W.J. Mortier, J. Phys. Chem., 88 (1984) 5752.
[141] T.J. Gluszak, D.T. Chen, S.B. Sharma, J.A. Dumesic and T.W. Root, Chem. Phys. Lett., 190 (1992) 36.
[142] D. Freude, H. Ernst and I. Wolf, Solid State Nucl. Magn. Reson., 3 (1994) 271.
[143] A.C. Kunwar, G.L. Turner and E. Oldfield, J. Magn. Reson., 69 (1986) 124.
[144] H. Schäfer, Diploma Thesis, University of Leipzig, 1987.
[145] H. Pfeifer, J. Chem. Soc., Faraday Trans. 1, 84 (1988) 3777.
[146] P.W. Anderson and P.R. Weiss, Jpn. J. Phys. Soc. 9 (1954) 316.
[147] B. Schneider, D. Doskocilova and J. Jakes, Proceedings of the XX Congress Ampere, Springer-Verlag, Berlin, 1976, p. 57.
[148] E.R. Andrew and A. Jasinski, J. Phys. C, 4 (1971) 391.
[149] C. Stephan, Diploma Thesis, Institute of Physics, University of Leipzig, 1988.
[150] L.W. Beck and J.F. Haw, J. Phys. Chem., 99 (1995) 1076.
[151] M. Hunger, unpublished results.